

1991

The Kinetics of Organic Matter Mineralization in Anoxic Marine Sediments

David J. Burdige
Old Dominion University, dburdige@odu.edu

Follow this and additional works at: https://digitalcommons.odu.edu/oeas_fac_pubs

 Part of the [Biogeochemistry Commons](#), and the [Oceanography Commons](#)

Repository Citation

Burdige, David J., "The Kinetics of Organic Matter Mineralization in Anoxic Marine Sediments" (1991). *OEAS Faculty Publications*. 137.
https://digitalcommons.odu.edu/oeas_fac_pubs/137

Original Publication Citation

Burdige, D.J. (1991). The kinetics of organic-matter mineralization in anoxic marine-sediments. *Journal of Marine Research*, 49(4), 727-761. doi: 10.1357/002224091784995710

The kinetics of organic matter mineralization in anoxic marine sediments

by **David J. Burdige**¹

ABSTRACT

The kinetics of sulfate reduction and inorganic nutrient production (ΣCO_2 , ammonium, and phosphate) were examined in the sediments at five sites in the southern Chesapeake Bay, using long term (>200 d) sediment decomposition experiments. Average first order rate constants for these processes (at 25°C) decreased from 8.2 to 3.7 yr⁻¹ in the surface sediments (0–2 cm), to 2.1 to 0.2 yr⁻¹ at 12–14 cm. The C/N and C/P ratios of the organic matter undergoing decomposition also increased with depth at these sites. Taken together, these results indicate that the reactivity of the organic matter undergoing mineralization decreases with depth in these sediments.

A model based on the multiple-G model for organic matter decomposition (hereafter referred to as the mixture model) was developed to examine the observed kinetics of all of these processes. As in the multiple-G model, the mixture model is based on the mineralization of organic matter in sediments occurring from distinct fractions of organic matter with differing reactivities. However here, differences in reactivity are indicated by differences in both the intrinsic rate constants for decomposition as well as the C/N or C/P ratios of the organic matter in the fractions. The mixture model was useful in interpreting the results of these experiments, and provided explanations for differences in the reactivity of organic matter in the surface sediments at these sites. It also appeared to provide information on the nature of the organic matter undergoing remineralization in these sediments, based on the predicted C/N or C/P ratios of these apparent fractions. The data from this study was also examined using the recently presented power model of Middelburg (1989). This analysis indicated the importance of pre-depositional decomposition in affecting the reactivity of sedimentary organic matter.

While all of these models provided insights into organic matter remineralization in marine sediments, they also all had mixed successes in describing (in a unified fashion) sulfate reduction and inorganic nutrient production in these southern Chesapeake Bay sediments. This observation indicates that care must be taken in interpreting information (e.g., rate constants, elemental ratios or apparent initial ages of the sedimentary organic matter) on organic matter in sediments, based on model derived parameters such as those that have been presented here. The ability to independently verify these model derived parameters of the sedimentary organic matter undergoing mineralization will likely be important in further refining these models and improving their usefulness in describing (and predicting) the factors controlling organic matter mineralization in marine sediments.

1. Department of Oceanography, Old Dominion University, Norfolk, Virginia, 23529-0276, U.S.A.

1. Introduction

The mineralization of organic matter in marine sediments has a significant impact on numerous biogeochemical processes in sediments and the water column. Since both the quantity as well as quality (or reactivity) of the sedimentary organic matter have been shown to affect the rates of these reactions (e.g., Westrich and Berner, 1984, 1988; Henrichs and Doyle, 1986; Emerson and Hedges, 1988; Middelburg, 1989; Murray and Kuivala, 1990), there is continuing interest in further elucidating the factors controlling these mineralization processes.

Efforts in this area have taken several approaches. Organic geochemical studies have begun to characterize sedimentary organic matter at the molecular or compound level (e.g., lipids, carbohydrates, amino acids; see Ertel and Hedges, 1985; Henrichs and Farrington, 1987; Haddad and Martens, 1988; Hamilton and Hedges, 1988; Burdige and Martens, 1988; Haddad, 1989; Martens *et al.*, 1991). Such information is of interest here since different biopolymers are known to have different reactivities with regards to their decomposition (Henrichs and Doyle, 1986). Several of these studies have also been able to quantify the mineralization of specific classes of organic compounds, and examine their decomposition in the context of overall sedimentary carbon and nitrogen cycling (Henrichs and Farrington, 1987; Burdige and Martens, 1988; Haddad and Martens, 1988). However in terms of understanding the controls on the mineralization of sedimentary matter such studies are generally limited by the lack of specific information on the types of macromolecules (or matrix) in which these individual compounds reside (e.g., see the discussion in Henrichs, 1991).

The mineralization of organic matter in marine sediments has also been studied by directly measuring the rates of processes such as sulfate reduction, methanogenesis, ammonium and phosphate production, as well as the turnover of small organic molecules such as acetate and amino acids (see Klump and Martens, 1983, Reeburgh, 1983, Skyring, 1987, and Capone and Kiene, 1988, for recent reviews). Rates of these processes have also been estimated using diagenetic models applied to both pore water and solid phase sedimentary profiles (Berner, 1980). These models often assume that there are two types of organic matter in marine sediments: a labile (or reactive) fraction, and a refractory fraction which appears to be essentially nonreactive on early diagenetic time scales. This formalism is based on a paper by Jørgensen (1978) in which he proposed that organic matter in marine sediments is actually composed of various groups of compounds that have different reactivities with regards to mineralization (in all further discussions this model will be referred to as the multiple-G model). Although other views of organic matter in sediments suggest that organic matter may better be described as a continuum with regards to its reactivity (see Middelburg, 1989, and the discussion below), the multiple-G model has in general proven quite successful in the study of the mineralization of sedimentary organic matter.

In an attempt to further examine the validity of the multiple-G model, Westrich and Berner (1984) carried out a series of long term decomposition experiments with Long Island Sound sediments in which they examined changes over time in particulate organic carbon concentrations and rates of bacterial sulfate reduction. Their results suggested that in these sediments organic matter mineralization by sulfate reduction was first order with respect to the organic matter undergoing decomposition, and that this organic matter was composed of two reactive fractions and one refractory fraction. There was an approximate order of magnitude difference in the reactivity of the two labile fractions of organic matter, based on the observed first order rate constants of 8 ± 1 and $0.94 \pm 0.25 \text{ yr}^{-1}$ for the decomposition of these two classes of sedimentary organic matter.

Similar rate constants for sulfate reduction and inorganic nutrient production have been determined in other nearshore and continental margin sediments (Nixon and Pilson, 1983; Westrich and Berner, 1984; Martens and Klump, 1984; Klump and Martens, 1987; Burdige and Martens, 1988; Jahnke, 1990; Murray and Kuivala, 1990; and others), using both diagenetic models and short term (several hour to up to ~ 1 week) whole sediment incubation techniques. Significantly lower rate constants for organic matter oxidation have also been observed in environments of these types, as well as in deep sea sediments (e.g., Emerson and Hedges, 1988; Murray and Kuivala, 1990; Middelburg, 1989). This then suggests that in the context of the multiple-G model that there are also higher order (i.e., less reactive) fractions of organic matter whose decomposition is significant (or observable) only on time scales longer than those of early diagenetic processes in most nearshore sedimentary environments.

In this paper, results will be presented from a series of long term anoxic sediment decomposition experiments using samples collected at five sites in the southern Chesapeake Bay and tributaries. The data from this study will be examined using both the multiple-G model and the recently presented power model of Middelburg (1989). The multiple-G model, as previously described for organic carbon oxidation and sulfate reduction, will be expanded here to examine nitrogen and phosphorus regeneration. These models and data will then be used to examine the kinetics of organic matter mineralization in these sediments and the factors controlling this process both in these and other anoxic marine sediments.

2. Materials and methods

a. Field sites. The sediments used in this study were collected at five sites in the southern Chesapeake Bay (see Fig. 1). Bottom water salinities at these site at the time of collection (August, 1988) ranged from $<10\text{‰}$ (st. 23) to $>30\text{‰}$ (st. 26). None of these stations showed evidence of bottom water anoxia at the time of sample collection, although station 17 in the Rappahanock River did have low bottom water oxygen concentrations ($43 \mu\text{M}$). A brief description of the physical and geochemical characteristics of the sediments at these five sites is listed in Table 1 and is primarily

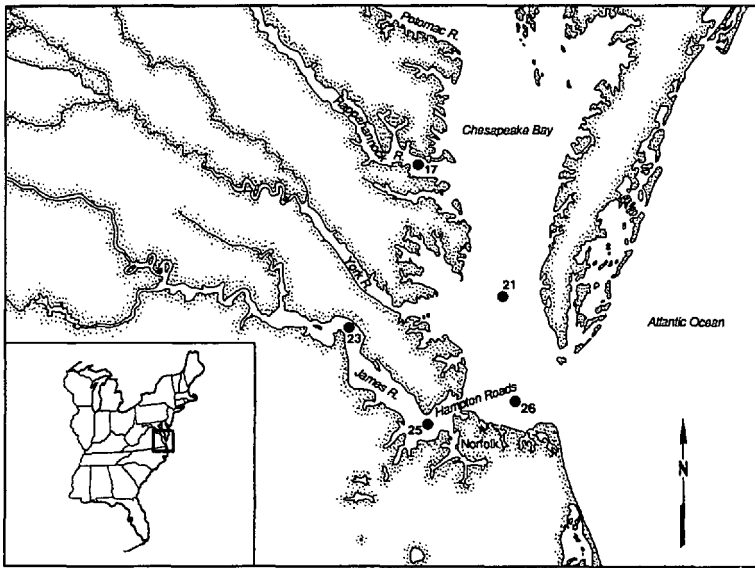


Figure 1. A map of the southern Chesapeake Bay and tributaries indicating the sites examined in this study. Additional information on the geochemical characteristics of these sites can be found in Table 1 and Burdige (1989a).

based on results reported in Burdige (1989a). These data are summarized here to aid in interpreting the results presented in this paper.

b. Experimental procedures. Sediment were collected by box core aboard the R/V *Linwood Holton*. These cores were sub-cored on the ship and returned to the lab (with water overlying the cores) where they were kept at 4°C until processed (approx. four weeks). Sediments slurries (sediment:seawater ratios of approx. 1:3 by weight) were prepared by mixing sediments from discrete 2 cm intervals of several cores with 0.2 μm filtered bottom water. For the station 23 experiments, the bottom waters were amended with sodium sulfate to a final sulfate concentration of approx. 20 mM, to avoid sulfate depletion. Slurry aliquots (10–15 ml) were dispensed into 20 ml serum bottles under N_2 in a Coy Anaerobic Chamber, crimp sealed, removed from the chamber and then incubated in the dark at 25°C in a constant temperature incubator. Bottles were periodically shaken by hand (every 3–4 days) to manually re-mix the slurries. Experiments are reported here by station number and ‘-1’ to indicate experiments with the 0–2 cm sediments, ‘-2’ for experiments with the 5–7 cm sediments and ‘-3’ for experiments with the 12–14 cm sediments.

Sampling over the 230 day time period of the experiments was accomplished by analyzing one set of bottles (one per station and depth interval) for each time point. The bottles were returned to the anaerobic chamber, and the slurry transferred from the serum bottle to a screw cap centrifuge tube. The samples were then centrifuged and the supernatant filtered through a 0.45 μm polycarbonate filter. The pH of the

Table 1. Geochemical characteristics of the sediments examined in this study.

Station ^a	BW salinities ^b	Sediment porosities ^c	TOC ^d	TN ^d	C/N ^d	TS ^d	TP ^d	Sediment description
17	18.9 (15.2)	0.85–0.92	3.10	3.69	9.8	11.9	0.72	fine silts; black color below 1 cm; these sediments are highly reducing with complete sulfate reduction occurring within 10 cm of the sediment-water interface.
21	27.3 (24.1)	0.45–0.64	0.66	0.39	19.8	2.45	0.62	silty clays; greenish grey at the surface (0–2 cm) becoming grey/black to black with depth. ^e
23	9.7 (6.9)	0.73–0.82	1.74	1.38	14.7	1.04	0.90	silty, clays; greenish/grey (0–7 cm) becoming grey/black with depth.
25	25.6 (19.7)	0.38–0.50	0.44	0.26	17.2	0.47	0.24	tan sands at the surface (0–3 cm), becoming grey/green to black with depth; with depth the sediments contain less sand and more silts and clays. ^e
26	30.4 (27.2)	0.48–0.63	0.60	0.40	19.3	1.53	0.52	silty clays; brown/grey at the surface (0–2 cm) becoming grey/black with depth. ^e

^aSee Figure 1 for a map showing the locations of these sites.

^bBottom water salinities (1 m off the bottom) measured in August, 1988. Salinities measured at these stations in April, 1988 are listed below these values in parentheses.

^cPorosity ranges over the upper 20 cm.

^dTOC = Organic Carbon (%); TN = Total Nitrogen (mg N/gdw); TS = Total Sulfur (mg S/gdw); TP = Total Phosphorus (mg P/gdw). These values are based on surface (0–1 cm) measurements made in cores collected at the same time as the sediments used in these experiments. The C/N ratios are molar ratios.

^eEvidence for bioturbation is seen in these cores, based on visual observations (e.g., snails, tube worms, faunal debris and/or animal sediment mounds found on the surfaces of the sediment cores).

waters was then determined. Samples for the analysis of ammonium and phosphate were acidified and frozen (-20°C) for later analysis. Samples for ΣCO_2 analyses were stored in crimp-seal vials with no head space and refrigerated (4°C) until analyzed, while samples for sulfate determinations were acidified and stored refrigerated until

analyzed. A portion of the residual sediment from the slurries was collected at the beginning and end of the experiments, frozen, and later analyzed of particulate (solid phase) organic carbon and total nitrogen.

c. Analytical procedures. Ammonium was determined colorimetrically using the phenol hypochlorite method, while phosphate was determined colorimetrically using the molybdate blue method (Gieskes and Peretsman, 1986). Sulfate was determined turbidometrically (Tabatabai, 1974; Burdige, 1989b). ΣCO_2 was determined by acidifying a sample with 1 N HCl to convert all of the inorganic carbon to $\text{CO}_2(\text{g})$, and then stripping this CO_2 out of the acidified sample with N_2 into the infrared detector of an Oceanography International Total Carbon Analyzer (Burdige, 1989b). Total carbon, nitrogen and sulfur in sediment samples were determined using a Carlo Erba NA 1500 Elemental Analyzer.

3. Results

The results of these experiments are shown in Figures 2 through 6. In general it can be seen that the concentrations of sulfate decreased, and ammonium, phosphate and ΣCO_2 increased in exponential-like fashions. At any given station, concentration changes were greatest in the surface sediments (0–2 cm) and smallest in the deeper sediments (12–14 cm).

To examine the kinetics of these processes the rates of sulfate reduction, and nutrient and ΣCO_2 production were assumed to be proportional to the amount of metabolizable carbon, nitrogen or phosphorus in the sediments. This assumption is discussed in part in the Introduction, and will also be discussed below in further detail. Given this assumption the following equation can be written,

$$\frac{dC_i}{dt} = \frac{k_i F}{1 + K_i} G_{m,i} \quad (1)$$

where: C_i is the concentration of ΣCO_2 , ammonium or phosphate in solution ($i = c, n$ or p respectively); t is time; k_i is the first order rate constant; $G_{m,i}$ is the concentration of metabolizable carbon, nitrogen or phosphorus; K_i is the reversible, equilibrium adsorption constant (ammonium and phosphate only); and F is a factor used to convert particulate concentrations (mg/L) to dissolved concentrations (e.g., μM). This last factor was determined using the porosity of the sediments and the amounts of water and wet sediment used in preparing the slurries. For sulfate, equation [1] is modified slightly to yield,

$$\frac{dC_s}{dt} = -\alpha k_i G_{m,i} \quad (2)$$

where α is the stoichiometric ratio of moles of sulfate reduced per mole of carbon oxidized, or ΣCO_2 produced (generally equal to $1/2$; see Eq. (6)). These equations can

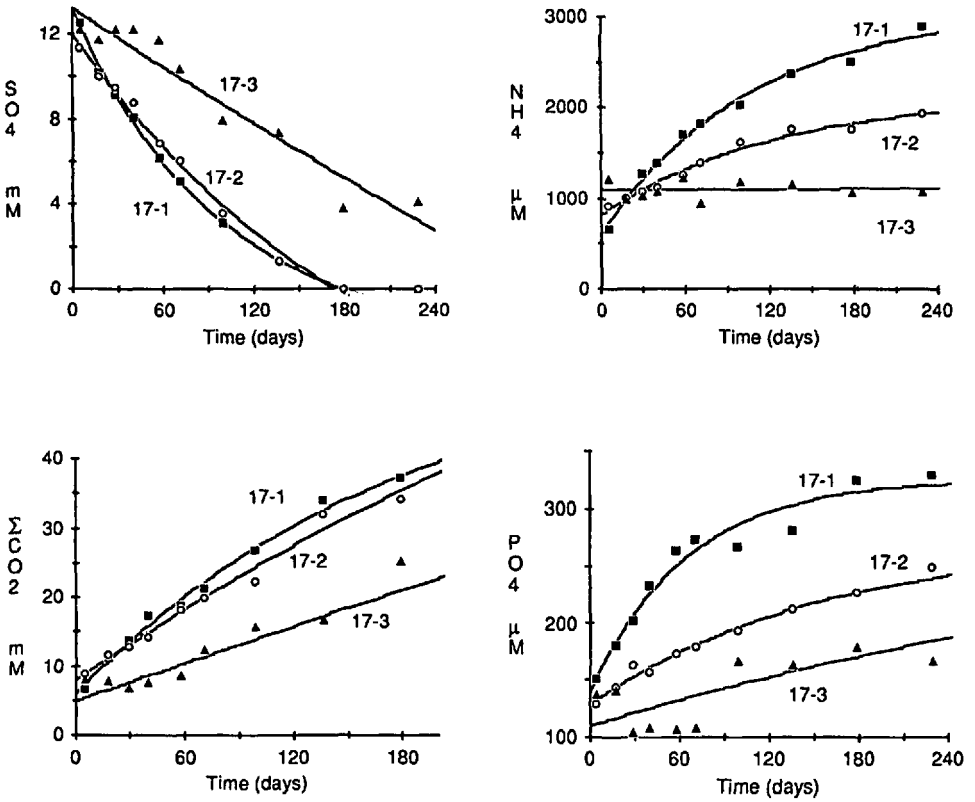


Figure 2. The results of the experiments carried out with sediments collected at station 17. The four figures represent the changes with time in either sulfate or inorganic nutrients in slurries prepared with sediments from the depths of 0–2 cm (17-1; filled squares), 5–7 cm (17-2; open circles) or 12–14 cm (17-3; filled triangles). The best fit curves through the data have been calculated with Eqs. (3)–(5) and the resulting best fit parameters are listed in Tables 2 and 3.

be solved by assuming $C_i = C_{o,i}$ at $t = 0$, yielding for ΣCO_2 ,

$$C_c = C_{o,c} + FG_{m,c}(1 - e^{-k_c t}) \tag{3}$$

for ammonium and phosphate,

$$C_i = C_{o,i} + \frac{FG_{m,i}}{1 + K_i}(1 - e^{-k_i t}) \tag{4}$$

and for sulfate,

$$C_s = C_{o,s} - \alpha FG_{m,c}(1 - e^{-k_s t}). \tag{5}$$

The data from these experiments were fit to these equations using the Simplex

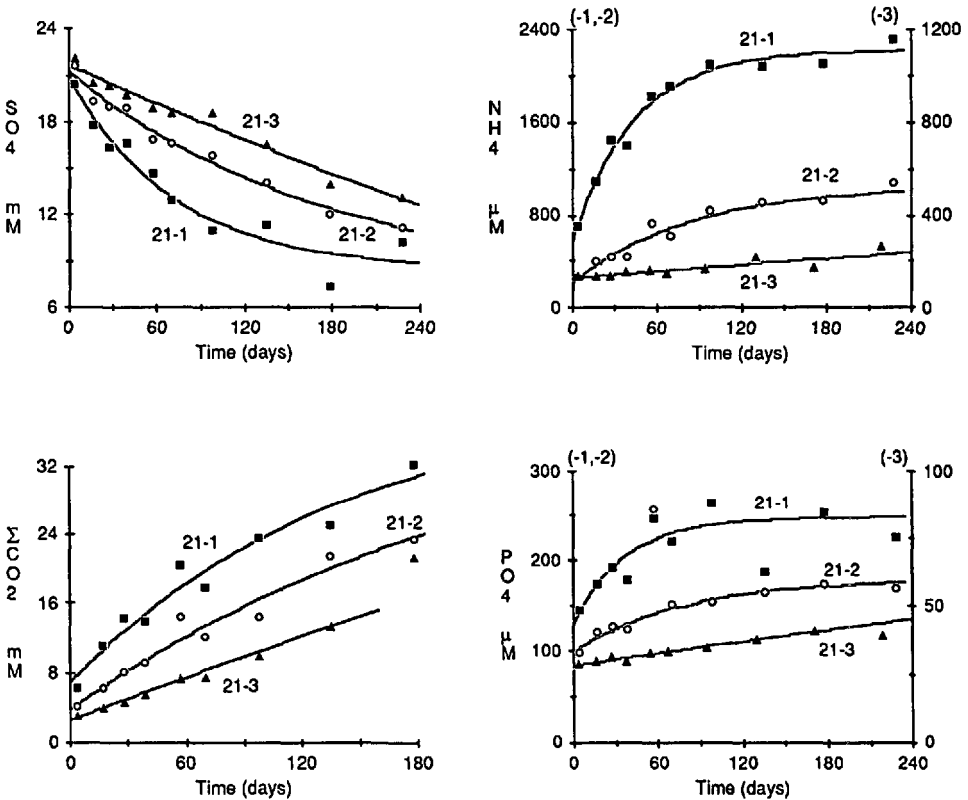


Figure 3. The results of the experiments carried out with sediments collected at station 21. The four figures represent the changes with time in either sulfate or inorganic nutrients in slurries prepared with sediments from the depths of 0–2 cm (21-1; filled squares), 5–7 cm (21-2; open circles) or 12–14 cm (21-3; filled triangles). Note the different concentration axes used for the ammonium and phosphate data from the 21-1 and the 25-2 and -3 experiments. The best fit curves through the data have been calculated with Eqs. (3)–(5) and the resulting best fit parameters are listed in Tables 2 and 3.

algorithm (Caceci and Cacheris, 1984) and the best fit k_i and $G_{m,i}$ values are listed in Tables 2 and 3. In all of the calculations in this paper, an ammonium adsorption coefficient (K_n) of 1.3 was used (Mackin and Aller, 1984) while a value of 1.2 was used for the phosphate adsorption coefficient (K_p ; Krom and Berner, 1980).

In the experiments with sediments from stations 17, 21 and 23 it can be seen that in any given experiment all four rate constants were approximately equal ($\pm \sim 30\%$; see Table 2). In contrast, stations 25 and 26 appeared to show a different type of behavior. Here (particularly in the surface sediments) the rate constants for ammonium and phosphate were generally significantly greater (up to an order of magnitude) than those for sulfate and ΣCO_2 . Neglecting for now these differences, it was also observed at all five stations that the average rate constants decreased with depth

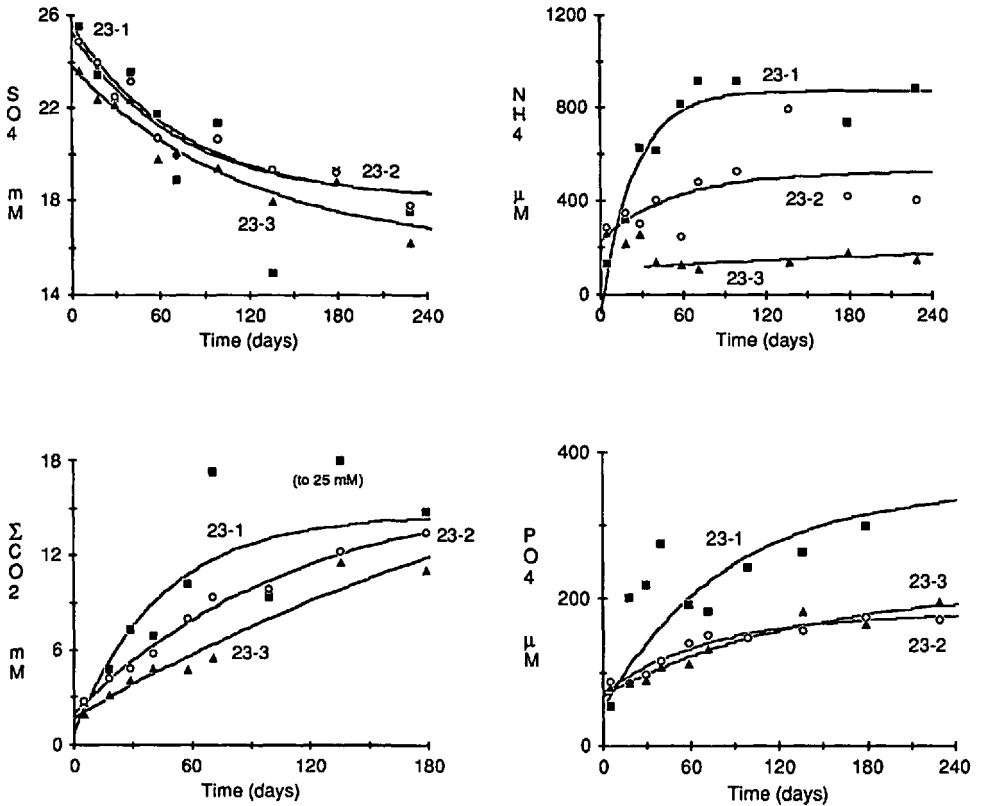


Figure 4. The results of the experiments carried out with sediments collected at station 23. The four figures represent the changes with time in either sulfate or inorganic nutrients in slurries prepared with sediments from the depths of 0–2 cm (23-1; filled squares), 5–7 cm (23-2; open circles) or 12–14 cm (23-3; filled triangles). The best fit curves through the data have been calculated with Eqs. (3)–(5) and the resulting best fit parameters are listed in Tables 2 and 3.

by about an order of magnitude (see Fig. 10). Lastly, it can be seen in Table 3 that the calculated, best fit values of metabolizable carbon, nitrogen and phosphorus ($G_{m,i}$) generally represented $<50\%$ of the measured organic carbon and total nitrogen and phosphorus in these sediments.

4. Discussion

The trends observed in these experiments are indicative of organic matter mineralization (ΣCO_2 , ammonium and phosphate production) occurring with bacterial sulfate reduction as the predominant “terminal” process. However, the use of the results of sediment slurry experiments such as these to quantify *in situ* parameters of organic matter mineralization in sediments depends on several factors. One is the

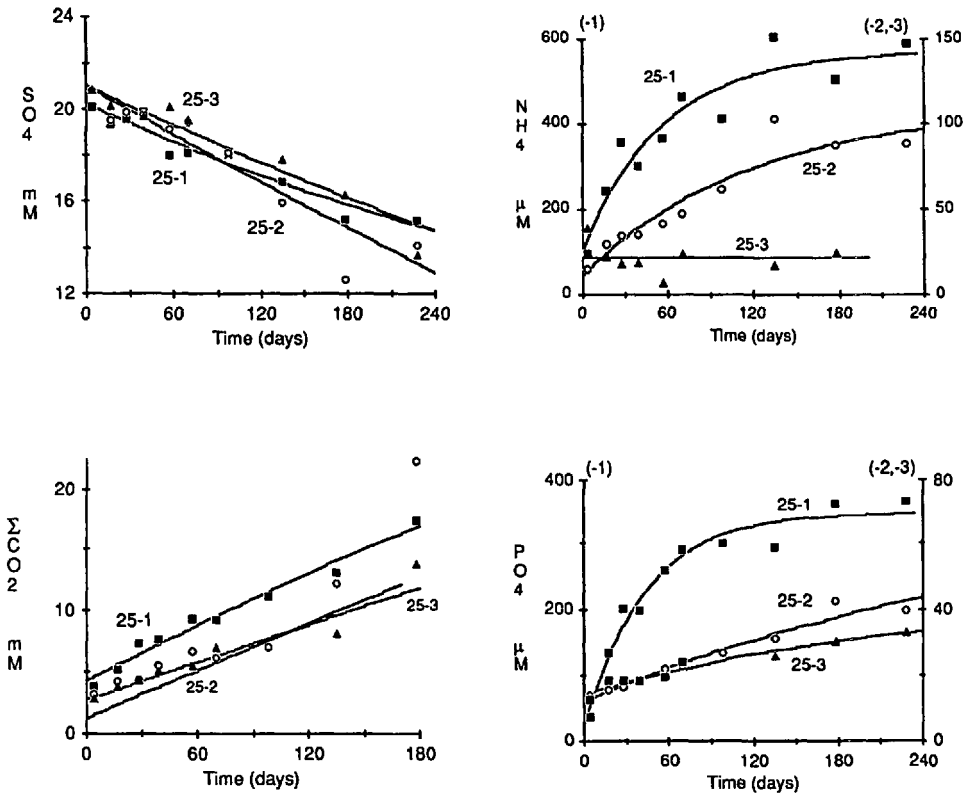


Figure 5. The results of the experiments carried out with sediments collected at station 25. The four figures represent the changes with time in either sulfate or inorganic nutrients in slurries prepared with sediments from the depths of 0–2 cm (25-1; filled squares), 5–7 cm (25-2; open circles) or 12–14 cm (25-3; filled triangles). Note the different concentration axes used for the ammonium and phosphate data from the 25-1 and the 25-2 and -3 experiments. The best fit curves through the data have been calculated with Eqs. (3)–(5) and the resulting best fit parameters are listed in Tables 2 and 3.

observation that while slurring decreases the measured rates of microbial processes (e.g., Jørgensen, 1978; Alperin and Reeburgh, 1985; Burdige, 1989b), the overall patterns (or pathways) of the microbial mineralization of sedimentary organic matter do not appear to be affected by the slurring procedure (Sørensen *et al.*, 1981; Christensen, 1984; Alperin and Reeburgh, 1985). In a study of sulfate reduction and ammonium production in mid-Chesapeake Bay sediments (Burdige, 1989b) it was also shown that the rates of these processes in sediment slurries were mathematically related to *in situ* rates in undisturbed sediments by a dilution factor which corrects the slurry rates for the dilution of the wet sediment with seawater. Based on these results it would therefore appear that slurring should affect kinetic equations such as Eqs. (1) and (2) primarily by decreasing the values of $G_{m,i}$, and should not affect the rate constants (k_i) determined with the results from these experiments.

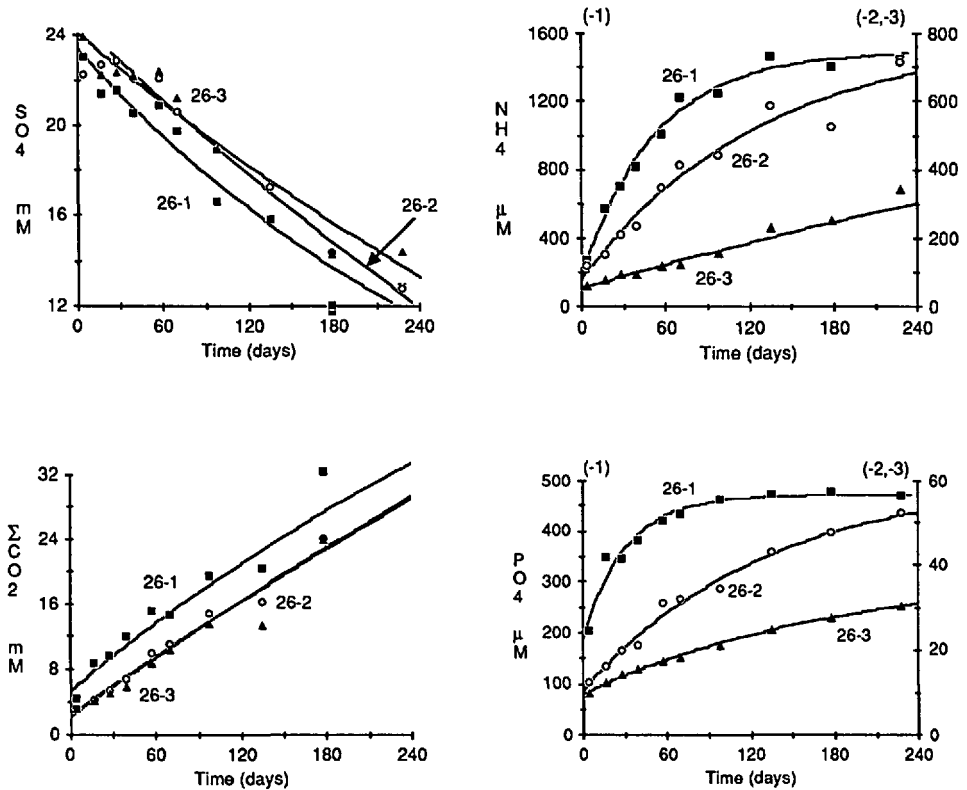


Figure 6. The results of the experiments carried out with sediments collected at station 26. The four figures represent the changes with time in either sulfate or inorganic nutrients versus time in sediment slurries prepared with sediments from the depths of 0–2 cm (26-1; filled squares), 5–7 cm (26-2; open circles) or 12–14 cm (26-3; filled triangles). Note the different concentration axes used for ammonium and phosphate data from the 26-1 and the 26-2 and -3 experiments. The best fit curves through the data have been calculated with Eqs. (3)–(5) and the resulting best fit parameters are listed in Tables 2 and 3.

The average rate constants for organic matter mineralization in these sediments ranged from $\sim 8 \text{ yr}^{-1}$ in the surface sediments to $< 0.2 \text{ yr}^{-1}$ at 12–14 cm (see Table 2). These values agree well with other rate constants for organic matter mineralization in nearshore, coastal and estuarine sediments (e.g., Nixon and Pilson, 1983; Westrich and Berner, 1984; Martens and Klump, 1984; Klump and Martens, 1987; Burdige and Martens, 1988; Middelburg, 1989), particularly when the rate constants determined here (at 25°C) are corrected to typical *in situ* sedimentary temperatures. This observation provides further evidence that the kinetic parameters determined in these sediment slurry experiments are likely accurate estimates of their true *in situ* values.

The importance of bacterial sulfate reduction in these experiments can be seen in

Table 2. Rate constants for organic matter remineralization in Southern Chesapeake Bay sediments.*

Expt.	Depth (cm)	k_s	k_c	k_p	k_n	Average
17-1	0-2	3.76	2.01	5.66	3.39	3.70 ± 1.30
17-2	5-7	1.72	0.77	2.34	2.88	1.93 ± 0.79
17-3	12-14	0.22	0.17	0.69	0.47	0.39 ± 0.21
21-1	0-2	5.13	2.42	9.86	8.40	6.45 ± 2.89
21-2	5-7	2.07	1.46	4.60	4.27	3.10 ± 1.36
21-3	12-14	0.37	0.16	0.09	0.30	0.23 ± 0.11
23-1	0-2	4.89	8.10	5.29	14.64	8.23 ± 3.90
23-2	5-7	5.11	3.18	5.07	6.68	5.01 ± 1.24
23-3	12-14	3.10	1.13	2.81	1.46	2.13 ± 0.84
25-1	0-2	0.80	0.51	8.40	6.42	4.03 ± 3.45
25-2	5-7	0.18	0.18	1.10	3.03	1.12 ± 1.16
25-3	12-14	0.35	0.39	1.64	0.00	0.80 ± 0.60
26-1	0-2	1.17	0.70	12.05	6.79	5.18 ± 4.63
26-2	5-7	0.49	0.28	2.70	2.77	1.56 ± 1.18
26-3	12-14	0.58	0.24	1.88	0.47	0.79 ± 0.64

All rate constants are yr^{-1} .

*These rate constants were obtained by fitting the data from these experiments to Eqs. (3)–(5).

Figure 7, where the concentrations of ΣCO_2 and sulfate in the experiments at each station are plotted against one another. Based on Eqs. (1) and (2) the slope of the line through these data (dC_c/dC_s) should equal $-1/\alpha$ (assuming for now that k_c and k_s are equivalent; see next section). As can be seen in this figure and in Table 4, the value of $\Delta\Sigma\text{CO}_2/\Delta\text{SO}_4^{2-}$ ($= -1/\alpha$) for these experiments are all 2 (within experimental error), the value expected if bacterial sulfate reduction predominates organic matter mineralization (and hence ΣCO_2 production; see Eq. (6) below). The occurrence in these experiments of sub-oxic respiratory processes that would be thermodynamically and kinetically favored over sulfate reduction (e.g., denitrification, iron or manganese reduction) could lead to $\Delta\Sigma\text{CO}_2/\Delta\text{SO}_4^{2-}$ ratios greater than 2. However dissolved nitrate, iron and manganese data from these experiments suggests that ΣCO_2 production from sub-oxic processes would affect this ratio by at most $\sim 1\%$ in the station 23 and 25 experiments and by $< 0.3\%$ in the other experiments (data not shown here).

a. The elemental composition of organic matter undergoing decomposition in these sediments. Stoichiometric models for nutrient regeneration under anoxic conditions (i.e., by sulfate reduction) assume that this process can be described by a simple

Table 3. Calculated values of metabolizable carbon, nitrogen and phosphorus, and measured values of total organic carbon, nitrogen and phosphorus in the sediments from these experiments.

Expt.	$G_{m,c}$ (a,b)	$G_{m,c}$ (a,c)	TOC (a,d)	TOC (a,e)	$G_{m,n}$ (a,f)	TN (a,d)	TN (a,e)	$G_{m,p}$ (a,f)	TP (a,e)	$G_{m,c}$ (g)	$G_{m,n}$ (g)	$G_{m,p}$ (g)
17-1	7.79	5.39	32.00	32.11	1.02	4.05	3.89	0.16	0.79	21%	26%	20%
17-2	10.84	5.99	29.94	33.19	0.44	3.56	3.90	0.10	0.82	27%	12%	12%
17-3	24.25	23.07	26.26	28.77	0.02	2.94	3.08	0.15	0.63	86%	1%	24%
21-1	0.47	0.36	18.59	6.49	0.06	1.92	0.42	0.01	0.62	3%	5%	1%
21-2	0.81	0.61	7.49	7.00	0.05	0.56	0.45	0.01	0.60	10%	9%	2%
21-3	2.77	1.34	14.50	7.25	0.02	1.02	0.42	0.02	0.53	19%	3%	5%
23-1	0.35	0.37	21.72	18.70	0.06	1.89	1.49	0.04	0.90	2%	4%	5%
23-2	0.52	0.49	23.34	21.39	0.03	1.92	1.71	0.02	0.85	2%	2%	3%
23-3	1.99	1.28	21.47	14.23	0.03	1.55	0.97	0.07	0.56	9%	2%	13%
25-1	3.05	1.70	15.16	3.85	0.07	0.75	0.27	0.10	0.23	25%	13%	43%
25-2	3.78	4.87	20.49	4.75	0.01	0.80	0.22	0.01	0.18	34%	3%	5%
25-3	1.68	2.29	23.38	3.72	0.00	0.90	0.14	0.01	0.21	15%	0%	3%
26-1	3.11	2.06	5.85	5.82	0.14	0.36	0.39	0.07	0.48	44%	38%	14%
26-2	6.33	4.38	7.81	5.98	0.06	0.59	0.41	0.01	0.50	78%	13%	2%
26-3	4.87	2.15	9.29	6.99	0.14	0.61	0.44	0.01	0.45	43%	26%	1%

(a) mg C/gds, mg N/gds or mg P/gds, as appropriate.

(b) Metabolizable organic carbon, based on fitting the ΣCO_2 data to Eq. (3).

(c) Metabolizable organic carbon, based on fitting the sulfate data to Eq. (5).

(d) Measured total carbon or nitrogen in the sediments from the first time point of this experiment.

(e) Measured total carbon, nitrogen or phosphorus in sediment cores collected at the same time the sediments used in this study were collected (from Burdige, 1989a).

(f) Metabolizable organic nitrogen or phosphorus (as appropriate), based on fitting the ammonium or phosphate data to Eq. (5).

(g) $G_{m,i}$ as a percentage of TOC, TN or TP (as appropriate).

'Redfield' type reaction (Richards, 1965),



although for several reasons this equation is clearly an oversimplification of this process. The majority of the ammonium and phosphate regeneration in anoxic environments likely does not directly occur during bacterial sulfate reduction, but rather appears to result from hydrolytic and/or fermentative processes that eventually produce H_2 and a small number of low molecular weight molecules such as acetate from complex sedimentary organic matter (Laanbroek and Veldkamp, 1982; Jacobsen *et al.*, 1987; Capone and Kiene, 1988; Burdige, 1991). The utilization of these compounds by sulfate reducing bacteria then results in the complete mineral-

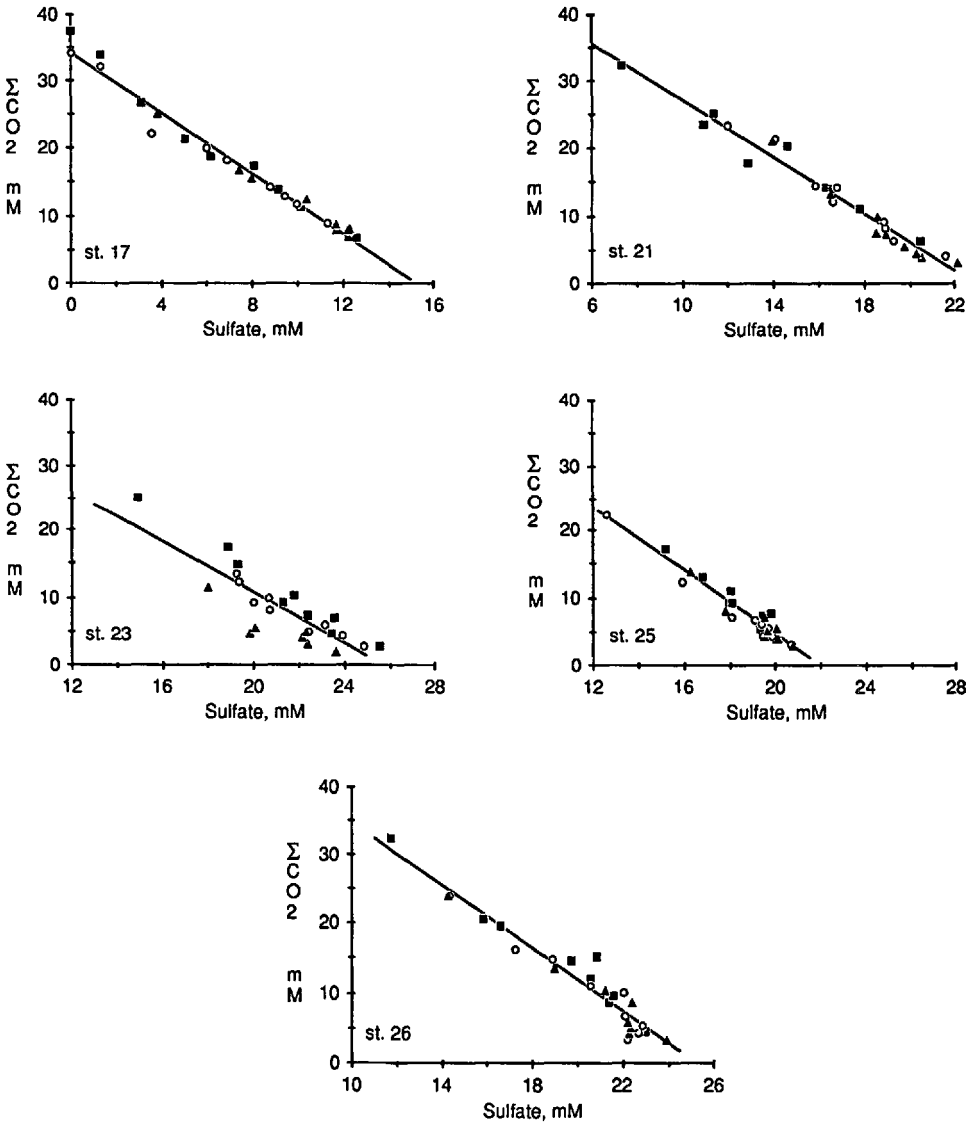


Figure 7. ΣCO_2 versus sulfate for the data from these experiments. For each station, the data from the three experiments have been plotted together (-1 experiments, filled squares; -2 experiments, open circles; -3 experiments, filled triangles). Also shown here are the best fit lines through the data, the slopes of which are listed in Table 4.

ization of sedimentary organic matter, with the sum of all of these processes being approximated by Eq. (6).

At the same time sedimentary C/N ratios generally increase with depth in many surficial coastal, marine and estuarine sediments (e.g., Klump and Martens, 1987). This is usually taken as an indication of preferential mineralization of more nitrogen-

Table 4. $\Delta\Sigma\text{CO}_2/\Delta\text{SO}_4^{2-}$ ($= 1/\alpha$) from the experiments of this study.

Station	$\Delta\Sigma\text{CO}_2/\Delta\text{SO}_4^{2-*}$
17	-2.24 ± 0.07
21	-2.11 ± 0.08
23	-1.90 ± 0.23
25	-2.36 ± 0.13
26	-2.27 ± 0.12

*For each station, this value is the slope of the best fit line determined from linear least squares fitting of the sulfate and ΣCO_2 data for all three experiments (see Fig. 7).

rich organic matter in sediments. In the context of the multiple-G model, this would also seem to imply that the more labile fractions of sedimentary organic matter have lower C/N ratios than that of bulk sedimentary organic matter (e.g., see Billen and Lancelot, 1988). Analogous arguments should hold for phosphorus mineralization and sedimentary C/P ratios, although processes such as authigenic mineral formation and adsorption of phosphate to iron oxides complicates the interpretation of sedimentary phosphorus profiles in this context (Berner, 1980; Krom and Berner, 1981; Klump and Martens, 1987).

To begin to further examine the relationships between sulfate reduction and inorganic nutrient production in anoxic sediments, the data from these experiments have been used to determine the elemental (C:N:P) ratios of the organic matter undergoing mineralization in these sediments. These elemental ratios have been estimated here in two ways. The first approach involves the use of the calculated $G_{m,i}$ values ($i = c, n$ or p) obtained from fitting the experimental data to Eqs. (3)–(5) (see Table 3). These ratios were also determined using concentration vs. concentration plots that are similar to those used above to determine the molar ratios $\Delta\Sigma\text{CO}_2/\Delta\text{SO}_4^{2-}$ from these experiments (e.g., Berner, 1977; Martens *et al.*, 1977; Elderfield *et al.*, 1981; Klump and Martens, 1987). These plots are shown in Figures 8 and 9 along with the linear least squares fit lines through the data. Based on Eqs. (1) and (2) and the assumption that $k_c = k_s = k_n = k_p$ (see paragraph below), these best fit slopes are then equal to,

$$\frac{dC_i}{dC_s} = \frac{-1}{\alpha} \frac{1}{1 + K_i} \frac{G_{m,i}}{G_{m,c}} = \frac{-1}{\alpha} \frac{1}{1 + K_i} \frac{1}{R_i} \quad (7)$$

where R_i is the C/N or C/P ratio of the organic matter undergoing mineralization. R_i values were calculated with this equation using dC_i/dC_s (the best fit slopes of the lines shown in Figs. 8 and 9), the values of $-1/\alpha$ listed in Table 4, and the previously discussed ammonium and phosphate adsorption coefficients.

Eq. (7) is also based on the assumption that all of the rate constants for these processes are equal (i.e., $k_s = k_c = k_p = k_n$) and therefore cancel one another out in the derivation of this equation. While this assumption appears to be true at stations

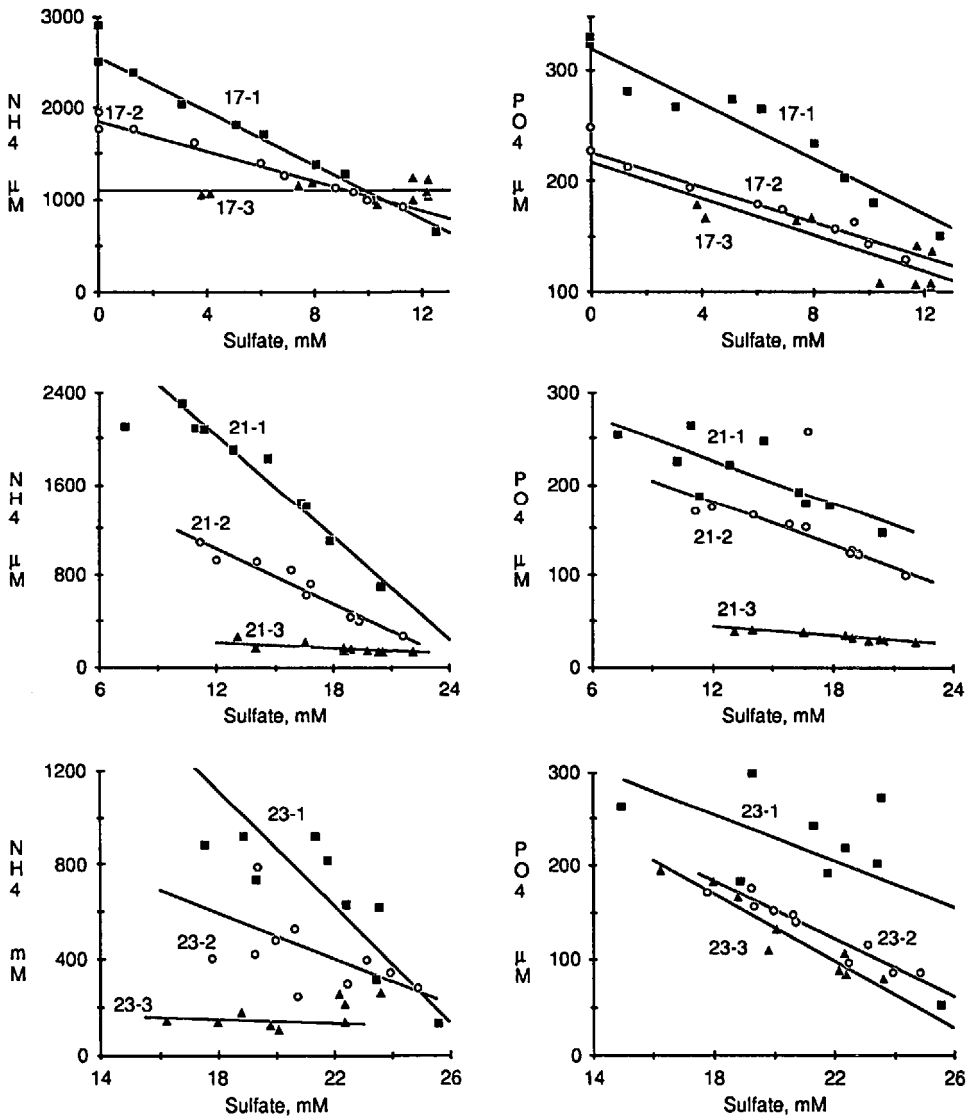


Figure 8. Ammonium and phosphate versus sulfate for the data from the station 17, 21 and 23 experiments (-1 experiments, filled squares; -2 experiments, open circles; -3 experiments, filled triangles). Also shown are the best fit lines through the data from each experiment. These slopes were used (as discussed in the text) in calculating the C/N and C/P ratios of the organic matter undergoing decomposition in these experiments (see Table 5).

17, 21 and 23, it does not appear so at stations 25 and 26 (see Table 2), particularly in the surface sediment. Since the kinetics of organic matter decomposition in the sediments of stations 25 and 26 are likely more complicated than that expressed by Eqs. (1)– (5) (see below), strictly speaking this also implies that the analysis of the

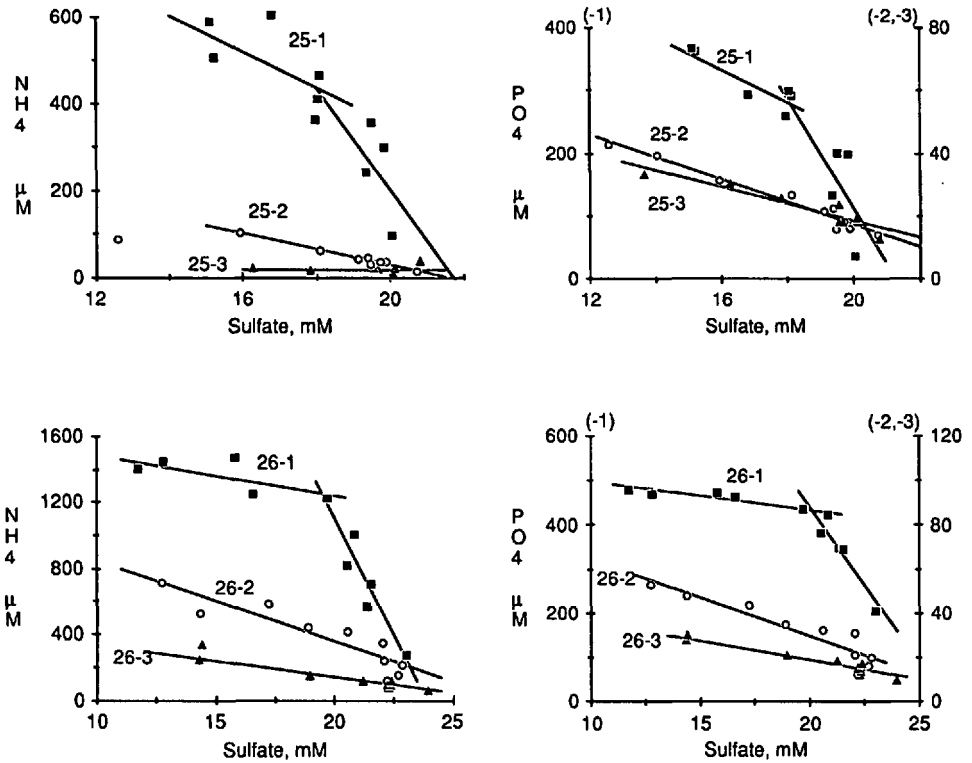


Figure 9. Ammonium and phosphate versus sulfate for the data from the station 25 and 26 experiments (-1 experiments, filled squares; -2 experiments, open circles; -3 experiments, filled triangles). Note the different concentration axes used for the phosphate data from the -1 and the -2 and -3 experiments. Also shown here are the best fit lines through the data from each experiment. As discussed in the text apparent changes in the C/N and C/P ratios of the organic matter undergoing remineralization in the -1 experiments have been estimated here by fitting this data to two straight lines. All of these slopes were used (as discussed in the text) in calculating the C/N and C/P ratios of the organic matter undergoing decomposition in these experiments (see Table 5).

data from these experiments with these equations is not correct. However in the following sections it will be shown how the equations presented here can be expanded to examine data from such experiments.

The elemental ratios calculated for each experiment are shown in Table 5. As can be seen in this table, the ratios calculated in the two manners described above generally agree quite well with one another. For station 17, 21 and 23 sediments the C/N or C/P ratios of the organic matter undergoing decomposition are generally constant in any given experiments (see Fig. 8 and Table 5). This would be expected if the mineralization of organic matter in a given sediment section occurs from one fraction of organic matter (an assumption that is actually implicit in Eqs. (1)–(5)). In contrast, it can also be seen in Figure 9 that these elemental ratios apparently change

Table 5. Elemental ratios of the organic matter undergoing remineralization in Southern Chesapeake Bay sediments.

Station/ expt.	Depth (cm)	C/P (conc. plot) [†]	C/P (curve fit) ^{††}	C/N (conc. plot) [†]	C/N (curve fit) ^{††}
17-1	0-2	81.0 ± 9.4	103.9 ± 18.9	6.7 ± 0.3	7.6 ± 1.4
17-2	5-7	129.2 ± 9.3	213.4 ± 61.4	12.0 ± 0.7	22.2 ± 6.4
17-3	12-14	271.1 ± 69.3	397.8 ± 9.9	1,840 ± 44,915	1,199 ± 30
21-1	0-2	117.8 ± 34.2	116.4 ± 16.2	6.1 ± 0.5	8.0 ± 1.1
21-2	5-7	119.5 ± 10.3	190.2 ± 26.5	11.5 ± 1.4	17.7 ± 2.5
21-3	12-14	578.0 ± 58.5	224.5 ± 78.2	117.8 ± 41.1	96.6 ± 33.6
23-1	0-2	69.2 ± 41.1	21.4 ± 0.4	6.7 ± 1.4	6.5 ± 0.1
23-2	5-7	56.5 ± 9.5	58.3 ± 1.9	17.1 ± 9.0	20.4 ± 0.723
23-3	12-14	48.6 ± 9.9	59.1 ± 12.8	181.8 ± 337.8	75.1 ± 16.3
25-1	0-2	12.3 ± 3.5 ⁱ 38.4 ± 8.7 ^f	61.2 ± 17.5	8.7 ± 2.0 ^j 24.7 ± 12.8 ^f	40.5 ± 11.6
25-2	5-7	297.7 ± 27.1	1,112 ± 140	56.5 ± 5.1	640.6 ± 80.92
25-3	12-14	396.7 ± 61.8	920 ± 142	10,921 ± 11,532	
26-1	0-2	14.5 ± 2.6 ⁱ 157.7 ± 33.8 ^f	100.5 ± 20.4	3.5 ± 0.7 ⁱ 41.0 ± 7.6 ^f	20.9 ± 4.2
26-2	5-7	295.3 ± 43.5	1,147 ± 209	20.1 ± 3.4	77.5 ± 14.1
26-3	12-14	600.8 ± 88.9	1,938 ± 751	51.7 ± 5.1	59.4 ± 23.0

All ratios are molar ratios.

[†]These ratios were calculated using Eq. (6) as discussed in the text (also see Figs. 8 and 9). For the surface sediment experiments at stations 25 and 26 (25-1 and the 26-1), 'i' and 'f' denote the ratios calculated with the initial and final slopes of the best fit lines shown in Figure 9.

^{††}These ratios were calculated with the best fit values of $G_{m,c}$, $G_{m,n}$ and $G_{m,p}$ (see Table 3) obtained by fitting the data from these experiments to Eqs. (3)-(5).

over the course of the 25-1 and 26-1 experiments. In these experiments it appears as if there are two fractions of organic matter undergoing successive decomposition, the latter fractions having higher C/N or C/P ratios. It is also in these experiments that the rate constants for phosphate and ammonium production are greater than those for either sulfate reduction or ΣCO_2 production (see Table 2 and the discussion above). The relationship of these observations to one another will be discussed below in greater detail. It is also interesting to note that the 25-2 and 26-2 experiments appear to show similar inequalities among rate constants (i.e., k_p and $k_n > k_c$ and k_s), yet plots of ammonium or phosphate versus sulfate are linear.

In the discussions in this paper it has also been assumed that the processes responsible for the observed concentration changes in these experiments are microbial, and related to the anoxic mineralization of sedimentary organic matter by bacterial sulfate reduction. However for phosphate the possibility also exists that some fraction of its observed production is also related to the release of adsorbed

phosphate during the reductive dissolution of iron oxides (see for example, Krom and Berner, 1981, and Klump and Martens, 1987, for a discussion of the effect of this process on phosphate cycling in nearshore marine sediments). Iron oxides are known to be strong adsorbers of phosphate (e.g., Krom and Berner, 1980), and in oxic sediments phosphate adsorption coefficients are significantly larger ($K > 50$) than values in anoxic sediments ($K \approx 1$ to 2).

It is not possible with the data presented here to unequivocally determine the relative roles of desorption versus microbial mineralization in causing the observed increases in phosphate concentrations. However several lines of evidence suggest that organic matter mineralization is primarily responsible. This conclusion is primarily based on observed similarities in nitrogen and phosphorus regeneration in these experiments, and the fact that ammonium adsorption and desorption, unlike phosphate, is not affected by changes in redox chemistry (i.e., dissolution of iron oxides).² At the same time, dissolved iron data from these experiments (data not shown here) suggest that the majority of the iron remobilization (or reduction) occurred in the first 20–30 days of these experiments, while changes in dissolved phosphate and ammonium occurred continuously during the 230 days of these experiments.

b. The reactivity of sedimentary organic matter with depth at these sites. It can be seen in Figure 10 and Table 5 that the elemental ratios of the organic matter undergoing decomposition generally increase with depth in these sediments. In the surface sediments the material undergoing decomposition appears to be close in composition to 'Redfield'-like organic matter ($C/N = 6.6$ and $C/P = 106$), while at depth this material becomes increasingly depleted in both nitrogen and phosphorus, leading to higher C/N and C/P ratios. At the same time, average rate constants for organic matter mineralization decrease with depth in these sediments (see Fig. 10). Taken together these observations provide evidence for the relationship between increasing C/N and C/P ratios and decreasing reactivity of organic matter.

Assuming that the deposition of organic matter has been constant at each of these sites over the age of the upper ~15–20 cm of sediments, these changes in k , C/N and C/P are likely related to mineralization processes occurring in the sediments.³ As

2. Specifically, this can be seen in the similarities in the k_p and k_r values (see Table 2), and in the trends with depth in the C/N and C/P ratios of the organic matter undergoing decomposition (see Table 5 and Fig. 10). These trends are also evident in the results of the 25-1 and 26-1 experiments, where both the phosphate and the ammonium data suggest that there were two fractions of organic matter undergoing decomposition in both experiments, with the second fractions having higher C/P and C/N ratios.

3. Variability with depth in the values of the ammonium and phosphate adsorption coefficients could also possibly lead to these observed changes with depth in the C/N and C/P ratios (e.g., see Eq. (7)). However given the K values used here, changes in K lead to roughly equivalent changes in elemental ratios (i.e., a $\pm 25\%$ change in K approximately translates into a $\pm 25\%$ change in either ratio). Given this observation, and the assumption that sedimentation patterns (i.e., sedimentation rates and sediment types) have been roughly constant at these five sites over the age of the upper 15–20 cm of sediments, it seems unlikely that the large changes with depth in the C/N and C/P ratios observed at all five sites are related to depth dependencies in the K values.

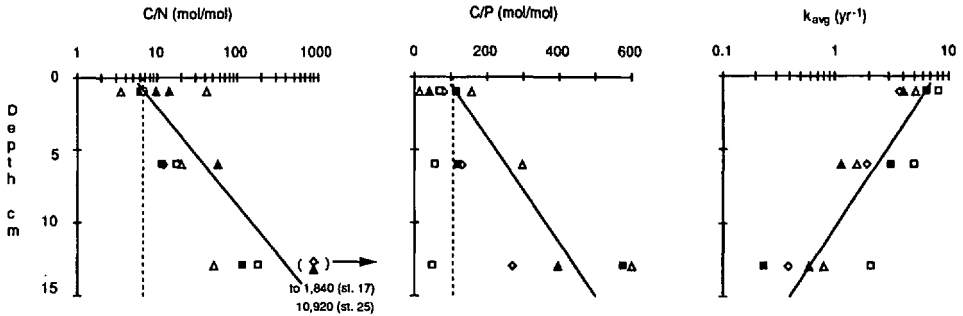


Figure 10. The C/N and C/P ratios and k_{avg} values of the organic matter undergoing decomposition, all versus depth, at stations: 17, open diamonds; 21, solid squares; 23, open squares; 25, filled triangles; 26, open triangles. Note the logarithmic scales for the C/N and k_{avg} axes and the linear scale for the C/P axis. Also shown on these figures (as dashed lines) are the Redfield C/N and C/P ratios. The rate constants shown here are taken from Table 2. The elemental ratios are those in Table 5 that are based on the values obtained from the concentration vs. concentration plots in Figures 7–9. The solid lines on each figure are included here solely to further illustrate the observed trends with depth in the data.

discussed above, the more labile organic matter in the surface sediments is apparently relatively enriched in N and P. As this material is consumed, mineralization processes at depth are fueled by increasingly less reactive organic matter which is also depleted in N and P. In the rest of this paper, two models that have previously been used to examine organic matter mineralization in sediments (i.e., the power model and the multiple-G model) will be used to further examine these transformations.

The exponential-like decrease with depth in the average rate constants in these sediments (Fig. 10) appears to be consistent with the power model for organic matter decomposition (Middelburg, 1989). This model is based on the assumption that there is a continuous decrease in the reactivity of sedimentary organic matter with time (or with depth in a sedimentary sequence). Using data ranging from laboratory experiments with “fresh” organic matter (e.g., recently collected plankton or algae) to field data from coastal, continental margin and pelagic sediments, Middelburg (1989) observed an empirical, inverse log-log relationship between the first order rate constant for organic carbon oxidation and time. This relationship appeared to be valid over eight orders of magnitude of time and rate constants. Unfortunately in the absence of quantitative information on sediment accumulation rates and mixing processes at these five sites in the southern Chesapeake Bay it is not possible to make a more explicit connection between sedimentary depths and the ages of the sediments used in this study. As such it is not possible to more carefully examine the depth dependence in the k values from this study with the power model.

These changes with depth in the reactivity of sedimentary organic matter at these sites can also be examined in the context of the multiple-G model. This analysis will

begin by examining these average rate constants from this study in the context of the results of Westrich and Berner (1984). In their experiments with Long Island Sound sediments, they obtained a k_1 of $8.0 \pm 1.0 \text{ yr}^{-1}$ for the most reactive fraction (G_1) of organic matter undergoing anoxic decomposition via sulfate reduction, and a k_2 of $0.94 \pm 0.25 \text{ yr}^{-1}$ for the next most reactive fraction (G_2). They also noted the existence of a third fraction of sedimentary organic matter (G_{NR}) which was nonreactive on the time scale of their experiments. In their paper Westrich and Berner (1984) suggested the possibility that their k_1 and k_2 values may be appropriate for describing the kinetics of organic matter oxidation by sulfate reduction in other marine sediments. With the results of the studies presented here, this hypothesis can be tested. In the analysis presented below differences in the sets of k 's for a given experiment (i.e., k_s and k_c vs. k_n and k_p) will initially be neglected. These differences will, however, be incorporated into the discussions in the next section.

Since the average rate constants for organic matter mineralization in these Chesapeake Bay surface sediments (0–2 cm) fall between the k_1 and k_2 values reported by Westrich and Berner (1984), one interpretation of these observations is that organic matter mineralization in these surface sediments occurs from mixtures of G_1 - and G_2 -type organic matter. The equation describing the production of ΣCO_2 from such a "mixture" of organic matter is then based on a modified form of Eq. (3).

$$C = C_o + FG_{m,c,1}(1 - e^{-k_1 t}) + FG_{m,c,2}(1 - e^{-k_2 t}) \quad (8)$$

where k_1 is assumed to be greater than k_2 . As can be seen in the example in Figure 11, mixtures of G_1 - and G_2 -type organic matter undergoing decomposition have "apparent" rate constants which are intermediate in value to the end-member k_1 and k_2 values. The magnitude of this apparent rate constant depends on the rate constants of the two end member fractions and the relative amounts of each fraction that are present. In such mixtures one does not necessarily observe the sequential utilization of each fraction, and to some extent both can be used simultaneously. However one may see the apparent sequential utilization of these fractions of organic matter if $k_1 \gg k_2$ and/or $G_{m,c,1} \gg G_{m,c,2}$. Re-examining the results of Westrich and Berner (1984) in the context of the mixture model (Eq. (8)) also suggests that their value of k_1 could possibly be an underestimate of its true value, if in their experiments they were also observing the decomposition of some mixture of G_1 - and G_2 -type organic matter. Evidence for this can be seen in the results of Klump and Martens (1987) as well as in the results presented here (see Table 2), in which rate constants greater than 8 yr^{-1} have been observed for the decomposition of sedimentary organic matter.

In the context of the mixture model and the k values of Westrich and Berner (1984) it would appear that with depth in these southern Chesapeake Bay sediments that G_1 -type material is eventually completely mineralized and that the decomposition of G_2 -type organic matter then appears to predominate. Finally, in the deeper

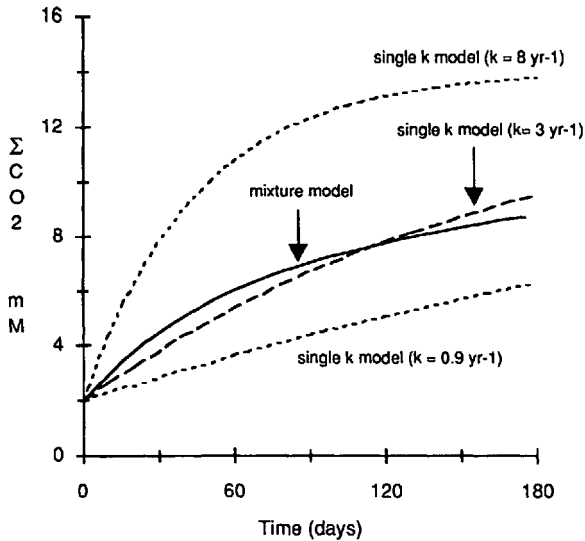


Figure 11. The production of ΣCO_2 versus time from organic matter with decomposition rate constants of: 8 yr^{-1} (upper short dashed line), 0.9 yr^{-1} (lower short dashed line) and 3 yr^{-1} (long dashed line). All were calculated using the single k model (i.e., Eq. (3)). Also shown is the production of ΣCO_2 versus time for the decomposition of a mixture of two types of organic matter (solid line) based on the mixture model Eq. (8). This mixture contains G_1 - and G_2 -type organic matter in a 1:2 ratio with the sum of these two fractions equalling the amount of organic matter in the three single k model examples. The k_1 for G_1 -type organic matter is assumed to be 8 yr^{-1} while the k_2 for G_2 -type material is 0.9 yr^{-1} .

sediments there is organic matter undergoing decomposition that appears to have a rate constant for mineralization that is lower than that reported by Westrich and Berner (1984) for G_2 -type organic matter. This suggests that in these sediments there is also a third fraction of organic matter that plays a role in the mineralization of sedimentary organic matter. Based on the results in Table 3 the rate constant (k_3) for this fraction is less than $\sim 0.2 \text{ yr}^{-1}$. Only an upper limit for k_3 can be established here, since it cannot be determined whether the observed kinetics of organic matter mineralization in the deep (12–14 cm) sediments is driven solely by the oxidation of G_3 -type material or a mixture of G_2 - and G_3 -type material.

This G_3 -type material is likely some fraction of the nonreactive organic matter (G_{NR}) in the experiments of Westrich and Berner (1984). The ability here to determine an upper limit for the rate constant of this apparent G_3 -fraction is based on differences in the experimental design of this study and that of Westrich and Berner (1984). Their study was performed with sediments from shallow depths (maximum depths of 6 cm) in which there was apparently significant amounts of labile (i.e., G_1 -type) organic matter. The almost two orders of magnitude difference in the rate constants for G_1 - and G_3 -type material would then preclude the ability to observe the kinetic of G_3 -type organic matter decomposition in the time of their

experiments. In contrast, the experiments performed here also used deeper sediments (12–14 cm) in which the more labile fractions of sedimentary organic matter had been removed (via mineralization) during the time of burial. This then allowed for the observation of the kinetics of decomposition of this more refractory sedimentary organic matter.

Although Westrich and Berner (1984) were not able to examine the kinetics of decomposition of this G_3 fraction, they discuss the fact that in many deeper anoxic, sediments sulfate reduction is supported by organic matter that is less reactive than G_2 -type material. The existence of such material is also expected based on observed rate constants for organic matter oxidation in certain nearshore, continental margin and deep-sea sediments (see the Introduction). The results presented here verify the occurrence and reactivity of this material.

c. The application of the mixture model to sedimentary nitrogen and phosphorus mineralization. While previous studies (e.g., Westrich and Berner, 1984; Middelburg, 1989) have begun to examine the factors controlling the reactivity of sedimentary organic matter, they have generally addressed this problem using information on sulfate reduction rates and/or rates of organic carbon mineralization. In contrast, the processes of nitrogen and phosphorus mineralization have not been examined using models such as the multiple-G model and/or the power model. Sedimentary nitrogen and phosphorus mineralization are usually modelled by assuming that the rate constants for sulfate reduction, and organic carbon, nitrogen and phosphorus mineralization are equivalent to one another and constant with depth in a given sedimentary environment (Berner, 1980). However this assumption may not always be true in all sediments (see, e.g., Table 2 and Klump and Martens, 1987). In light of these observations, the relationship between sulfate reduction, and ΣCO_2 , ammonium and phosphate production will be further examined using the results from this study and the mixture model described above.

This analysis will begin with the results of the experiments with surface sediments from stations 25 and 26 (experiments 25-1 and 26-1), in part because they yielded results which appeared to be very different from those of the other experiments of this study. First, the values of k_n and k_p in these experiments were significantly larger than those of k_s and k_c from the same experiments (see Table 2). Concentration vs. concentration plots also suggested that there were two 'fractions' of organic matter undergoing sequential decomposition in these experiments (see Fig. 9). Taking these differences in the rate constants at face value implies that the rates of nitrogen and phosphorus mineralization in these sediments are faster than the rates of sulfate reduction (or ΣCO_2 production). Such a situation would then lead to changes in the "apparent" C/N or C/P ratios of the organic matter undergoing decomposition over the course of the experiment with these sediments (see Fig. 12). Unfortunately, this "explanation" of the observed differences of these rate constants is somewhat

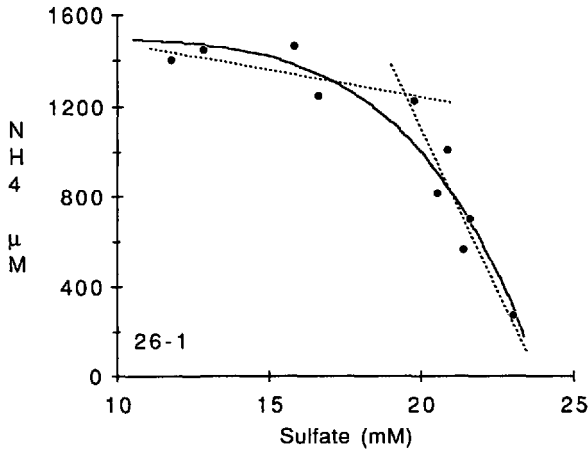


Figure 12. Ammonium versus sulfate for the data from the 26-1 experiment (filled circles). The two dashed straight lines are the same as those shown in Figure 10 for this data. The solid curve represents the plot of the best fits to the ammonium and sulfate data (versus time; see Fig. 6), here plotted against one another. As is discussed in the text, differences in the rates of ammonium production and sulfate reduction in this experiment (expressed here as differences in the best fit k_c and k_n values) lead to the observed apparent changes in the C/N ratio of the material undergoing remineralization.

incomplete, as it does not provide a sufficiently mechanistic explanation (in the context of the previous discussions) for the coupling of nitrogen and phosphorus mineralization to sulfate reduction and organic carbon oxidation in these experiments.

To quantify this coupling, the mixture model (Eq. (8)) has been expanded here by assuming that the two different fractions of organic matter undergoing mineralization also have different C/N or C/P ratios. In light of the previous discussion the more reactive fraction of organic matter is assumed to have both a larger k value as well as a lower C/N and C/P ratio. For ammonium and ΣCO_2 production Eq. (8) can be re-written,

$$[\Sigma\text{CO}_2] = [\Sigma\text{CO}_2]_o + FG_{m,c,1}(1 - e^{-k_1t}) + FG_{m,c,2}(1 - e^{-k_2t}) \quad (9)$$

$$[\text{NH}_4] = [\text{NH}_4]_o + \frac{FG_{m,n,1}}{1 + K_n}(1 - e^{-k_1t}) + \frac{FG_{m,n,2}}{1 + K_n}(1 - e^{-k_2t}) \quad (10)$$

where k_1 is greater than k_2 and $(\text{C/N})_1 [= G_{m,c,1} / G_{m,n,1}]$ is also less than $(\text{C/N})_2 [= G_{m,c,2} / G_{m,n,2}]$. For brevity, future discussions will only present the application of this model to sedimentary carbon and nitrogen mineralization, although analogous relationships also exist for carbon and phosphorus. It should also be noted that in developing this model to examine the results of the surface sediment (0–2 cm) experiments, the potential importance of G_3 and other higher order (i.e., lower

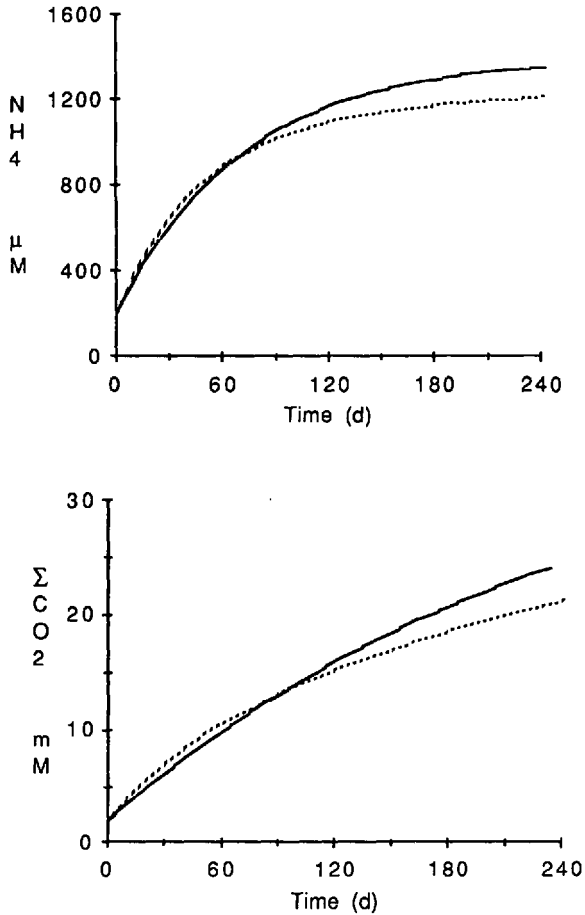


Figure 13. The production of ammonium (above) and ΣCO_2 (below) versus time from organic matter having a k_c of 1.5 yr^{-1} , a k_n of 5 yr^{-1} and a C/N ratio of 13 (solid line). These curves were calculated using the single k model equations (i.e., Eqs. (3) and (4)). Also shown is the production of ammonium and ΣCO_2 from a mixture of two fractions of organic matter having the following properties: $k_1 = 8 \text{ yr}^{-1}$, $(\text{C/N})_1 = 3$, $k_2 = 0.9 \text{ yr}^{-1}$ and $(\text{C/N})_2 = 40$ (dashed line). These curves were calculated using the mixture model equations (9) and (10). The amounts of metabolizable carbon and nitrogen in these two examples were chosen such that the amounts of either quantity in the single k model example were equal to their sums in the two fractions used in the mixture model example.

reactivity) fractions of organic matter has been neglected. On the time scales of these experiments, this material can be considered to be 'nonreactive' and therefore does not likely affect (to any significant extent) the kinetics of organic matter mineralization in surface sediments.

An example of the production of ammonium and ΣCO_2 from such a mixture of sedimentary organic matter is shown in Figure 13. As in the example in the previous

section (Fig. 11, where the mixture model was applied solely to organic carbon oxidation), nutrient production from such mixtures can also be approximately described by equations based on the single k model (e.g., Eqs. (3)–(5)). The apparent average C/N ratio of the organic matter undergoing decomposition in this single k model example (based on the $G_{m,n}$ and $G_{m,c}$ values) is also intermediate between the C/N ratios of the two fractions in the mixture model. In addition plots of ammonium versus sulfate using either of these examples show curvature as in Figure 12. Such trends can also be seen in the data from the 26-1 and perhaps in the 25-1 experiments (see Table 5), in that the C/N and C/P ratios based on the curve fitting parameters $G_{m,i}$ are intermediate between the ratios predicted by fitting the concentration vs. concentration plots to two straight lines.

In this example in Figure 13, as in the previous example in Figure 11, the k values here from the single k model (now both k_c and k_n) are again intermediate between the end-member rate constants of the two fractions undergoing decomposition. However now because of differences in the C/N ratios of the two fractions of organic matter undergoing decomposition, it is also observed that k_n is not equal to, and is actually larger than, k_c . Ammonium production in this example occurs mostly from the decomposition of G_1 -type material, since G_1 nitrogen is 73% of the total ($G_1 + G_2$) metabolizable nitrogen. This then results in k_n being closer in magnitude to k_1 than to k_2 . Conversely, since carbon mineralization occurs predominantly from this G_2 -type material, k_c is therefore closer to k_2 than to k_1 (in this example 83% of the total metabolizable carbon is found in the G_2 -type material).

In summary then, in the single k model (i.e., Eqs. (3)–(5)), k_c and k_n are assumed to be linked by stoichiometric (or redox) considerations, based on the oxidation of sedimentary organic carbon being coupled ultimately to sulfate reduction. However in a sediment where there are two types of organic matter undergoing decomposition, k_n and k_p need not equal k_c and k_r . Using the mixture model to examine these systems, such differences in rate constants (i.e., k_n , k_p , k_c and k_r) appear to be caused by two factors: differences in the intrinsic rate constants (k_1 and k_2) of the two fractions; and differences in the relative amounts of the total C, N and P mineralization occurring from each of the fractions undergoing decomposition (which is dependent in part on both the amounts of each fraction present and the C/N [or C/P] ratios of each fraction).

d. The factors controlling organic matter mineralization in southern Chesapeake Bay sediments. In this section the mixture model presented above and the power model of Middelburg (1989) will be used to begin to examine the factors controlling organic matter mineralization in the surface sediments of these five sites.

To carry out this analysis, the data from the 25-1 and 26-1 experiments were initially re-fit to the mixture model equations (Eqs. (9) and (10)) as follows. The C/N ratios of the two fractions were assumed to be those determined by the concentration

vs. concentration plots in Figure 9 (also see Table 5), while the amount of metabolizable nitrogen in the first fraction ($G_{m,n,1}$) was determined from the difference between the initial ammonium concentration in the experimental slurry and the ammonium concentration at which the two straight lines in the ammonium versus sulfate plots in Figure 9 cross one another. This approach is based on the assumption that this slope break is indicative of a change (from G_1 to G_2) in the fraction of organic matter which predominates the overall mineralization process. Given these three values (C/N_1 , C/N_2 and $G_{m,n,1}$), the ammonium and ΣCO_2 data from the 25-1 and 26-1 experiments were then fit to Eqs. (9) and (10) using the Simplex algorithm to obtain best fit values of k_1 , k_2 and $G_{m,n,2}$ (note that by fixing the C/N ratios of the two fractions of organic matter, the two $G_{m,c,i}$ values can be calculated using these ratios and the $G_{m,n,i}$ values).

The sulfate and the ammonium data from these experiments were also fit in this way to Eq. (10) and a modified form of Eq. (9), where $[\Sigma\text{CO}_2]_o$ was replaced by $[\text{SO}_4^{2-}]_o$ and the two $FG_{m,c,i}$ parameters replaced by $-\alpha FG_{m,c,i}$. The errors listed in Table 6 for the k_1 and k_2 values are then based on the averages of the two sets of best fit parameters obtained from fitting the data of each experiment. Also listed in Table 6 are the value of $G_{m,n,i}$ and $G_{m,c,i}$ as percentages of $G_{m,i,1} + G_{m,i,2}$. The reasons for presenting these values in this fashion will be discussed below.

In Table 5 it can be seen that the C/N ratios of the two apparent fractions of organic matter undergoing decomposition in the 25-1 and 26-1 experiments are slightly different. The extent to which these differences are real, and their effect on the interpretation of these calculations, will be discussed below. However in using Eqs. (9) and (10) to examine the data from these experiments the two set of C/N ratios were also averaged and the average ratios then used in fitting the data from the 25-1 and 26-1 experiments to the mixture model. In this second case all of the other relevant parameters ($G_{m,n,i}$, $G_{m,c,i}$, k_i) were determined as discussed above.

The results of fitting the data from the 25-1 and 26-1 experiments to the mixture model equations are summarized in Table 6. The best fit to the data from 26-1 experiment with the mixture model is also shown in Figure 14, along with the fit to the data using the single k model (Eqs. (3)–(5)). Reasonably good fits to the data are obtained using both models. As in the example in Figure 13, the k_n values from the fits to the 25-1 and 26-1 data with the single k model (see Table 2) are both closer in magnitude to k_1 than k_2 (see Table 6). Again, this occurs because the majority of the metabolizable nitrogen in the surface sediments of stations 25 and 26 is in the G_1 fraction ($\sim 70\%$). Similarly, since the majority of the metabolizable carbon in these sediments is in the G_2 fraction, the apparent k_c or k_s values from the single k model are closer in magnitude to k_2 than k_1 . It is also interesting to note that the best fit k values determined here for the G_1 and G_2 fractions ($k_1 \sim 7.3 \text{ yr}^{-1}$ and $k_2 \sim 1.1 \text{ yr}^{-1}$) agree very well with analogous values (8 ± 1 and $0.94 \pm 0.25 \text{ yr}^{-1}$) determined by Westrich and Berner (1984). This then suggests that their rate constants may indeed

Table 6. A summary of the results obtained from fitting the data from the surface sediment experiments to the mixture model equations.

Station	C/N ₁ (molar)	C/N ₂ (molar)	k_1 (yr ⁻¹)	k_2 (yr ⁻¹)	$G_{m,e,1}$ (a)	$G_{m,n,1}$ (a)
25-1 (b)	8.7	24.7	6.2 ± 0.6	2.0 ± 0.7	30%	55%
26-1 (b)	3.5	41.0	8.2 ± 0.3	0.69 ± 0.02	18%	72%
(avg. values)	6.1	32.9	7.2 ± 0.5	1.3 ± 0.7		
25-1 (c)	6.1	32.9	7.7 ± 0.4	1.1 ± 0.02	24%	64%
26-1 (c)	6.1	32.9	7.3 ± 1.1	0.62 ± 0.08	39%	78%
			7.5 ± 1.0	0.86 ± 0.28		
17-1 (26-1 values, d)					15%	67%
(average values, e)					48%	83%
21-1 (26-1 values, d)					25%	80%
(average values, e)					41%	88%
23-1 (26-1 values, d)					24%	78%
(average values, e)					54%	86%

(a) $G_{m,i,1}$ as a percentage of $G_{m,i,1} + G_{m,i,2}$.

(b) The C/N values used here were based on the best fits to the data from these experiments shown in Figure 10. The values of k_1 , k_2 , $G_{m,n,1}$, $G_{m,n,2}$, $G_{m,e,1}$ and $G_{m,e,2}$ were then determined as discussed in the text.

(c) The C/N values used here were based on the averages of the C/N ratios for the G_1 and G_2 fractions observed in the 25-1 and 26-1 experiments. All of the other parameters were then determined as discussed in the text.

(d) The data from these experiments were fit using the C/N₁ and k_i values obtained from fitting the data from the 26-1 experiment. All of the other parameters were then determined as discussed in the text.

(e) The data from these experiments were fit using the average C/N ratios (6.1 and 32.9) and k values (7.5 and 0.86 yr⁻¹) obtained from fitting the data from the 26-1 and 25-1 experiments. All of the other parameters were then determined as discussed in the text.

be appropriate for the two most reactive fractions of organic matter in anoxic, coastal marine sediments.

An examination of the C/N ratios of the G_1 - and G_2 -type organic material predicted by these experiments (~3 to 8 and ~25 to 40, respectively) also allows for an estimation of the types of organic compounds which comprise these fractions of sedimentary organic matter. Material in the G_1 -fraction with this low C/N ratio could be indicative of proteinaceous material, since the more 'commonly' occurring amino acids in nature (e.g., aspartic acid, glutamic acid, serine, glycine, alanine, valine and leucine) have C/N ratios of 2 to 6. Proteins and hydrolyzable amino acids in natural samples (marine sediments or particulate material in the oceans) also have C/N ratios ranging from 3.7 to 4.2 (Lee and Cronin, 1982; Burdige and Martens, 1988). The G_2 -type organic matter could be composed of vascular plant materials, as they generally have C/N ratios that are greater than 20 (e.g., Ertel and Hedges, 1985; Haddad, 1989). While this discussion is not meant to imply that only these biochemi-

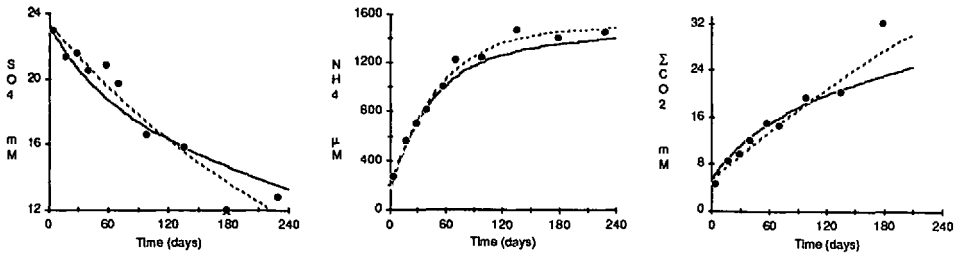


Figure 14. Sulfate reduction, and ammonium and ΣCO_2 production versus time in the 26-1 experiment. The dashed lines in the figures are the fits to the data with the single k model (Eqs. (3)–(5)), using the best fit parameters listed in Tables 2 and 3 (note that these curves are also shown in Fig. 3). The solid lines are the best fits to the data using the mixture model equations (9) and (10) assuming: $k_1 = 8.2 \text{ yr}^{-1}$, $(\text{C/N})_1 = 3.5$, $k_2 = 0.69 \text{ yr}^{-1}$ and $(\text{C/N})_2 = 41$. The procedures used to determine these parameters are discussed in the text. It should also be noted that similar agreements were also obtained for the 25-1 data using the 25-1 C/N ratios, and for both data sets (25-1 and 26-1) using the average C/N ratios (see Table 6).

cals make up G_1 - and G_2 -type organic matter in these (or any other) marine and estuarine sediments, previous studies of the geochemistry of these compounds in marine sediments do appear to be qualitatively consistent with these suggestions. This discussion is also presented here in part to indicate a possible linkage between studies of the organic geochemistry of sediments (see the Introduction) and studies of organic matter diagenesis based on inorganic nutrient data and diagenetic models.

Using the two sets of k and C/N values from the 25-1 and 26-1 experiments, the data from the three other surface sediment experiments were also re-fit using the mixture model. These data were fit to the mixture model equations in two ways: (1) using the C/N ratios and the k values determined from fitting the data from the 26-1 experiment; and (2) using the average C/N ratios and k values obtained with both the 25-1 and 26-1 data. Using either set of parameters there were then two quantities ($G_{m,n,1}$ and $G_{m,n,2}$) obtained in fitting these data to the mixture model equations. $G_{m,c,1}$ and $G_{m,c,2}$ were then determined with these $G_{m,n,i}$ values and the appropriate C/N ratios. The results of fitting these data with the mixture model equations is summarized in Tables 6 and 7. Examining the fitting parameters from the single k model and the mixture model suggests that for these five sites there is a positive correlation between $\%G_{m,c,1}$ and k_{cs} ($r = 0.82$ for the simple linear regression). In contrast the $\%G_{m,n,1}$ and k_n values from these sites are much less strongly correlated ($r = 0.36$).

Given these observations it appears that the relative amounts of carbon and nitrogen in the G_1 or G_2 fractions plays an important role in determining the apparent rate constants (k_c , k_s [or k_{cs}] and k_n) for the mineralization of organic matter in the surface sediments at these sites. When $\%G_{m,n,1}$ and $\%G_{m,c,1}$ values are high (i.e., stations 17, 21 and 23), the observed rate constants k_{cs} and k_n for these mixtures are both approximately equal, although they intermediate between the end-member k_1 and k_2 values (see Tables 2 and 7). It also appears that in the ranges of $\%G_{m,c,1}$ and

Table 7. A comparison of selected parameters obtained from fitting the data from the surface sediment experiments to the three models for organic matter remineralization discussed in the text

Station	Single k model [†]			Mixture model ^{††}		Power model [*]
	k_{cs}	k_n	k_{avg}	% $G_{m,c,1}$	% $G_{m,n,1}$	a (yr ⁻¹)
23-1	6.50 ± 1.60	14.64	8.23	54%	86%	0.05 ± 0.01
21-1	3.78 ± 1.36	8.40	6.45	41%	88%	0.13 ± 0.07
17-1	2.89 ± 0.88	3.39	3.70	48%	83%	0.23 ± 0.12
26-1	0.94 ± 0.24	6.79	5.18	39%	78%	0.96 ± 0.16
25-1	0.66 ± 0.14	6.42	4.03	24%	64%	1.13 ± 0.38

[†]The k_{cs} values are based on the averages of the k_c and k_i values listed in Table 2. The k_n and k_{avg} values here are taken from Table 2.

^{††}% $G_{m,i,1}$ is $G_{m,i,1}$ as a percentage of $G_{m,i,1} + G_{m,i,2}$. These values are taken from Table 6 and are based on fits to the data using the 25-1 and 26-1 average C/N and k_i values.

^{*} a (the apparent initial age of the sedimentary organic matter) was calculated as discussed in the text using the sulfate and ΣCO_2 data from these experiments. The values (and errors) reported here are based on the averages of the two a values determined for each experiment.

% $G_{m,n,1}$ found in these surface sediments (24 – 54% and 64 – 86% respectively) that the k_{cs} values are more strongly correlated to % $G_{m,c,1}$ than the k_n values are to % $G_{m,n,1}$ (see discussion above). This then leads to an apparent “uncoupling” of carbon and nitrogen mineralization in the sediments with the lowest % $G_{m,c,1}$ values (i.e., stations 25 and 26; see Table 7).

The ability to observe these differences in k_{cs} and k_n values, or the C/N ratios of the two fractions of organic matter undergoing mineralization, also depends on the overall length of the experiment. For example if the 26-1 experiment had only been run for ~ 60 days (at which point sulfate would only have decreased to ~ 20 mM) the importance of the mineralization of G_2 -type organic matter would not have been seen in these experiments (see Figs. 6 and 9). Similarly if the 17-1, 21-1 and 23-1 experiment had been run for longer time periods (increasing the overall importance of G_2 mineralization in the latter portions of these experiments) it is likely that the concentration vs. concentration plots shown in Figure 8 would have shown the type of curvature seen in Figure 9.

Differences in the reactivity of organic matter in these surface sediment may also be examined using the power model of Middelburg (1989). In the development of his model Middelburg (1989) defines a parameter “ a ” called the apparent initial age of the sedimentary organic matter. This parameter is meant to quantify the extent to which sedimentary organic matter has undergone pre-depositional mineralization. In his analysis of literature data, a was found to vary from 0.09 d in fresh plankton, to 0.26 yr in the sediments of Cape Lookout Bight to 14–35,000 yr in pelagic sediments of the central Pacific.

Using the sulfate and ΣCO_2 data from the experiments reported here, the

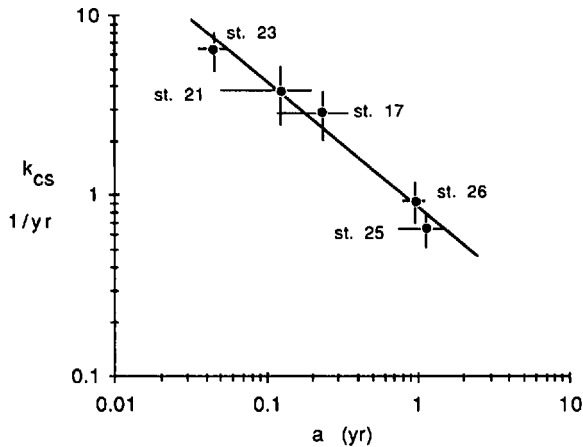


Figure 15. The apparent initial age (a) of the organic matter undergoing remineralization in the surface (0–2 cm) sediments of the five sites of this study versus k_{cs} , the average of the rate constants for sulfate reduction (k_r) and ΣCO_2 production (k_p) in these surface sediments. The k_{cs} and a values were calculated as discussed in the text and are listed in Table 7. The best fit line through this log-log transformation of the data is included here to indicate the negative correlation between the two parameters, and is not meant to imply any functional relationship.

apparent initial ages of the organic matter in the surface sediments at these sites were calculated using a modified form of Eq. (11) in Middelburg's (1989) paper. As can be seen in Table 7 and Figure 15, a strong negative correlation is observed between k_{cs} and a ($r = 0.98$ for the log-log plot shown in Fig. 15). Longer apparent initial ages leads to lower rate constants for sulfate reduction and ΣCO_2 production in surface sediments of the southern Chesapeake Bay. This result is consistent with other observations in the literature that the reactivity of sedimentary organic matter is strongly affected by the nature and extent of pre-depositional degradation of this organic matter (e.g., Martens *et al.*, 1991). It is also interesting to note that a negative correlation exists between the apparent initial ages of the surface sedimentary organic matter at these sites and the relative percentages of either metabolizable carbon and nitrogen in the G_1 fraction (see Table 7). In this context it appears (as would be expected) that pre-depositional degradation also leads to preferential mineralization of G_1 -type organic matter, causing the relative percentage of this fraction to decrease as the length of pre-depositional degradation increases.

e. Concluding Remarks. At five sites in the southern Chesapeake Bay and tributaries, average rate constants (at 25°C) for sulfate reduction, and ΣCO_2 , ammonium and phosphate production decreased from 8.2 to 3.7 yr^{-1} in the surface sediments (0–2 cm), to 2.1 to 0.2 yr^{-1} at 12–14 cm (see Table 2 and Fig. 10). The C/N and C/P ratios of the organic matter undergoing decomposition also increased with depth

(see Table 5 and Fig. 11). Assuming that the deposition of organic matter at each of these sites has been constant over the age of the upper ~ 20 cm of sediments these results indicate that the reactivity of organic matter undergoing mineralization in these sediments decreased with depth, presumably as the more reactive components are selectively utilized.

A model based on the multiple-G model (the mixture model) was developed to examine the observed kinetics of sulfate reduction and inorganic nutrient production in these sediments. With the mixture model it was seen that when two apparent types of organic matter are undergoing decomposition in a sediment, the observed kinetics of sulfate reduction or inorganic nutrient production from such a mixture are similar to that predicted by the decomposition of a single fraction of organic matter whose characteristics are intermediate to those of the two end-members. In the mixture model differences in the reactivity of each fraction are expressed by differences in the k and C/N (or C/P) values for each fraction. This model was shown to be useful in interpreting the results of the experiments with surface sediments, and suggested that observed differences in the reactivity of organic matter in these sediments was a function of the relative amounts of the two types of organic matter undergoing decomposition. It was also shown how the mixture model might provide information on the nature of the organic matter undergoing mineralization in these sediments, based on the predicted C/N or C/P ratios of the two fractions of organic matter undergoing decomposition.

The data from this study were also examined using the power model of Middelburg (1989). This analysis indicated the importance of pre-depositional decomposition in affecting the reactivity of sedimentary organic matter. Unfortunately it is not currently possible to apply the power model to the examination of nitrogen and phosphorus mineralization in sediments, as the parameters in the power model equations reported by Middelburg (1989) were derived primarily using organic carbon concentration and sulfate reduction rate data. In light of this observation, it would be interesting to carry out an analysis similar to that described by Middelburg (1989) for nitrogen and phosphorus diagenesis.

While all of these models provided insights into the process of organic matter mineralization in marine sediments, they also all had mixed successes in describing (in a unified fashion) sulfate reduction and inorganic nutrient production in these southern Chesapeake Bay sediments (and other sedimentary environments as well). For example, at the present time it is not possible to determine whether differences in the sets of k and C/N values for G_1 - and G_2 -type organic matter at stations 25 and 26 are indeed real. Resolution of questions such as this one are important for many reasons, in part because they relate to the issue of whether it is indeed possible to uniquely define common G_1 - and G_2 -types of organic matter for these and/or other anoxic marine and estuarine sediments (based on their intrinsic rate constants and C/N, or C/P, values). This observation further reinforces arguments put forth by

Middelburg (1989) that care must be taken in interpreting information (e.g., rate constants and elemental ratios) on different fractions of organic matter in sediments, based on model fit parameters such as those that have been presented here.

As discussed above, organic geochemical studies of the major biochemicals found in marine sediments may in part continue to provide information that will be useful in making more substantive connections between such "apparent" rate constants, elemental ratios, and ages, and their true values, based on the more direct observation of the biochemical composition of the organic matter actually undergoing mineralization in a sediment. With such information, along with more detailed information on the rates and mechanisms of these mineralization processes, it should then be possible to continue to refine these models and improve their usefulness in describing (and predicting) the factors controlling carbon, nitrogen and phosphorus mineralization in marine and estuarine sediments.

Acknowledgments. I would like to thank several people, including Barbara Mowery, Juli Homstead, Jeff Gardner, Robert Williamson, Anne James and Surya Dhakar, for help with the laboratory and field work of this project. I would also like to thank Greg Cutter, Iris Anderson, Val Klump and an anonymous reviewer for critically reading earlier versions of this manuscript. Discussions with Walter Boyton, Jeff Cornwell, Dominic Di Toro, Mike Kemp and Pete Sampou were also very important in the initial planning of these experiments. This work was primarily supported by grants from the EPA/Chesapeake Bay program, with additional financial support for preparing this manuscript provided by NSF grant OCE-8817409.

REFERENCES

- Alperin, M. J. and W. S. Reece. 1985. Inhibition experiments on anaerobic methane oxidation. *Appl. Environ. Microbiol.*, *50*, 940-945.
- Berner, R. A. 1977. Stoichiometric models for nutrient regeneration in anoxic marine sediments. *Limnol. Oceanogr.*, *22*, 781-786.
- 1980. *Early Diagenesis. A Theoretical Approach*. Princeton University Press, Princeton, NJ.
- Billen, G. and C. Lancelot. 1988. Modelling benthic nitrogen cycling in temperate coastal ecosystems, in *Nitrogen Cycling in Coastal Marine Environments*, T. H. Blackburn and J. Sørensen. eds., J. Wiley and Sons, 341-378.
- Burdige, D. J. 1989a. 1988 Sediment Monitoring Program for the Southern Chesapeake Bay. ODURF Technical Report 89-6.
- 1989b. The effects of sediment slurring on microbial processes, and the role of amino acids as substrates for sulfate reduction in anoxic marine sediments. *Biogeochemistry*, *8*, 1-23.
- 1991. Microbial processes affecting alanine and glutamic acid in anoxic marine sediments. *FEMS Microbiol. Ecology*, *85*, 211-231.
- Burdige, D. J. and C. S. Martens. 1988. Biogeochemical cycling in an organic-rich marine basin-10. The role of amino acids in sedimentary carbon and nitrogen cycling. *Geochim. Cosmochim. Acta*, *52*, 1571-1584.
- Caceci, M. S. and W. P. Cacheris. 1984. Fitting curves to data. *Byte*, *9*, 340-362.

- Capone, D. G. and R. P. Kiene. 1988. Comparison of microbial dynamics in marine and freshwater sediments: Contrasts in anaerobic carbon catabolisms. *Limnol. Oceanogr.*, *33*, 725–749.
- Christensen, D. 1984. Determination of substrates oxidized by sulfate reduction in intact cores of marine sediments. *Limnol. Oceanogr.*, *29*, 189–192.
- Elderfield, H., R. J. McCafrey, N. Luedtke, M. Bender and V. W. Truesdale. 1981. Chemical diagenesis in Narragansett Bay sediments. *Amer. J. Sci.*, *281*, 1021–1055.
- Emerson, S. and J. I. Hedges. 1988. Processes controlling the organic carbon content of open ocean sediments. *Paleocean*, *3*, 621–634.
- Ertel, J. R. and J. I. Hedges. 1985. Sources of sedimentary humic substances: vascular plant debris. *Geochim. Cosmochim. Acta*, *49*, 2097–2107.
- Gieskes, J. M. and G. Peretsman. 1986. Water chemistry procedures aboard the JOIDES RESOLUTION—some comments. Ocean Drilling Program. TAMU. Tech. Note No. 5
- Haddad, R. I. 1989. Sources and reactivity of organic matter accumulating in an anoxic marine sediment. Ph.D thesis, Univ. of North Carolina, Chapel Hill.
- Haddad, R. I. and C. S. Martens. 1988. Biogeochemical cycling in an organic-rich marine basin-9. Sources and fluxes of vascular plant derived organic material. *Geochim. Cosmochim. Acta*, *51*, 2991–3001.
- Hamilton, S. E. and J. I. Hedges. 1988. The comparative geochemistries of lignins and carbohydrates in an anoxic fjord. *Geochim. Cosmochim. Acta*, *52*, 129–142.
- Henrichs, S. M. 1991. Early diagenesis of organic matter in marine sediments: progress and perplexity. *Mar. Chem.*, (in press).
- Henrichs, S. M. and A. P. Doyle. 1986. Decomposition of ¹⁴C-labelled organic substrates in marine sediments. *Limnol. Oceanogr.*, *31*, 765–778.
- Henrichs, S. M. and J. W. Farrington. 1987. Early diagenesis of amino acids and organic matter in two coastal marine sediments. *Geochim. Cosmochim. Acta*, *51*, 1–15.
- Jacobsen, M. E., J. E. Mackin and D. G. Capone. 1987. Ammonium production in sediments inhibited with molybdate: implications for the sources of ammonium in anoxic marine sediments. *Appl. Environ. Microbiol.*, *53*, 2435–2439.
- Jahnke, R. A. 1990. Early diagenesis and recycling of biogenic debris at the seafloor, Santa Monica Basin, California. *J. Mar. Res.*, *48*, 413–436.
- Jørgensen, B. B. 1978. A comparison of methods for the quantification of bacterial sulfate reduction in coastal marine sediments. 1. Measurements with radiotracer techniques. *Geomicrobiol. J.*, *1*, 11–27.
- Klump, J. V. and C. S. Martens. 1983. Benthic nitrogen regeneration, in *Nitrogen in the Marine Environment*, E. J. Carpenter and D. G. Capone, eds., Academic Press, 411–457.
- 1987. Biogeochemical cycling in an organic-rich marine basin-5. Sedimentary nitrogen and phosphorus budgets based upon kinetic models, mass balances, and the stoichiometry of nutrient regeneration. *Geochim. Cosmochim. Acta*, *51*, 1161–1173.
- Krom, M. D. and R. A. Berner. 1980. Adsorption of phosphate in anoxic marine sediments. *Limnol. Oceanogr.*, *25*, 797–806.
- 1981. The diagenesis of phosphorus in a nearshore marine sediment. *Geochim. Cosmochim. Acta*, *45*, 207–216.
- Laanbroek, H. J. and H. Veldkamp. 1982. Microbial interactions in sediment communities. *Phil. Trans. Royal Soc. London B*, *297*, 533–550.
- Lee, C. and C. Cronin. 1982. The vertical flux of particulate organic nitrogen in the sea: decomposition of amino acids in the Peru upwelling area and the equatorial Atlantic. *J. Mar. Res.*, *40*, 227–251.

- Mackin, J. E. and R. C. Aller. 1984. Ammonium adsorption in marine sediments. *Limnol. Oceanogr.*, *29*, 250–257.
- Martens, C. S., R. A. Berner and J. K. Rosenfeld. 1977. Interstitial water chemistry of anoxic Long Island Sound sediments. 2. Nutrient regeneration and phosphate removal. *Limnol. Oceanogr.*, *23*, 605–617.
- Martens, C. S., R. I. Haddad and J. P. Chanton. 1991. Organic matter accumulation, remineralization and burial in an anoxic marine sediment, *in* Productivity, accumulation and preservation of organic matter in recent and ancient sediments, J. K. Whelan and J. W. Farrington, eds., (in press).
- Martens, C. S. and J. V. Klump. 1984. Biogeochemical cycling in an organic-rich marine basin-4. An organic carbon budget for sediments dominated by sulfate reduction and methanogenesis. *Geochim. Cosmochim. Acta*, *48*, 1987–2004.
- Middelburg, J. J. 1989. A simple rate model for organic matter decomposition in marine sediments. *Geochim. Cosmochim. Acta*, *53*, 1577–1581.
- Murray, J. W. and K. M. Kuivala. 1990. Organic matter diagenesis in the northeast Pacific: transition from aerobic red clay to suboxic hemipelagic sediments. *Deep-Sea Res.*, *37*, 59–80.
- Nixon, S. W. and M. E. Q. Pilson. 1983. Nitrogen in estuaries and coastal marine ecosystems, *in* Nitrogen in the Marine Environment, E. J. Carpenter and D. G. Capone, eds., Academic Press, 565–648.
- Reeburgh, W. S. 1983. Rates of biogeochemical processes in anoxic sediments. *Ann. Rev. Earth Planet. Sci.*, *11*, 269–298.
- Richards, F. A. 1965. Anoxic basins and fjords, *in* Chemical Oceanography, vol. 1, J. P. Riley and G. Skirrow, eds., Academic Press, 611–645.
- Skyring, G. W. 1987. Sulfate reduction in coastal ecosystems. *Geomicro. J.*, *5*, 295–374.
- Sørensen, J., D. Christensen and B. B. Jørgensen. 1981. Volatile fatty acids and hydrogen as substrates for sulfate-reducing bacteria in anaerobic marine sediments. *Appl. Environ. Microbiol.*, *42*, 5–11.
- Tabatabai, M. A. 1974. A rapid method for determination of sulfate in water samples. *Environ. Letters*, *7*, 237–243.
- Westrich, J. T. and R. A. Berner. 1984. The role of sedimentary organic matter in bacterial sulfate reduction: The G model tested. *Limnol Oceanogr.*, *29*, 236–249.
- 1988. The effect of temperature on rates of sulfate reduction in marine sediments. *Geomicrobiol. J.*, *6*, 99–117.